UNIVERSITÀ DEGLI STUDI
DI GENOVA

26 testXpo
FORUM FOR MATERIALS TESTING
October 16-19, 2017 at Zwick in Ulm

Experimental approaches for mechanical investigation of soft biological tissues as meniscal cartilage

Alberto Lagazzo

Department Of Civil, Chemical and Environmental Engineering - Dicca, University of Genoa, Italy
Dicca-Zwick/Roell - Material Science Joint Laboratory – Biomedical Engineering Section – Unige

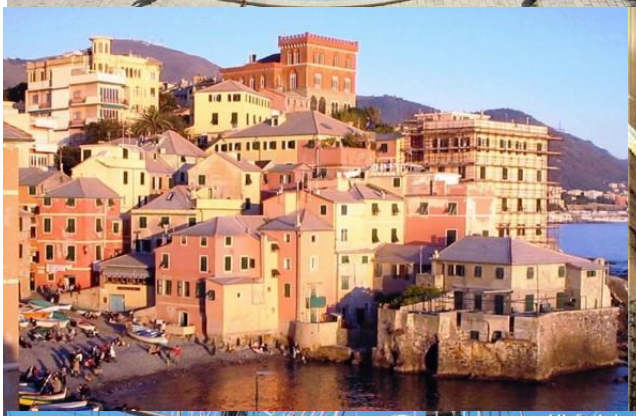

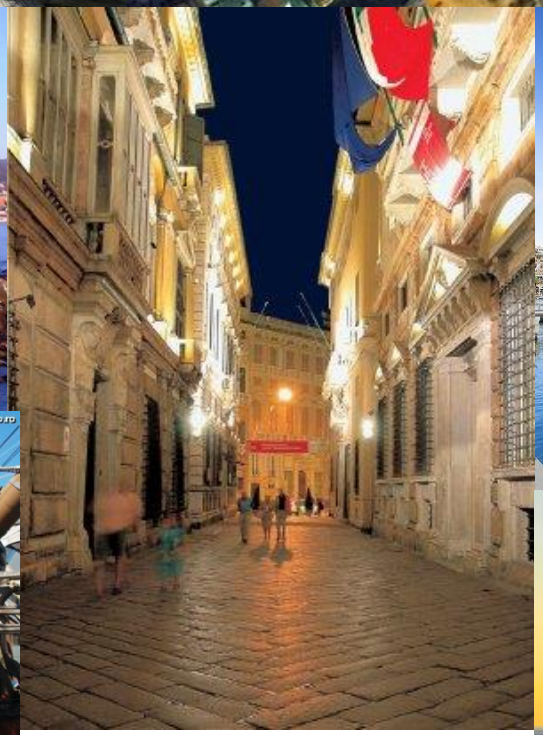

Genova

DICCA – Zwick/Roell Joint Laboratory

Zwick / Roell

Mechanical equipment DICCA – Zwick/Roell Lab

Max load 50KN

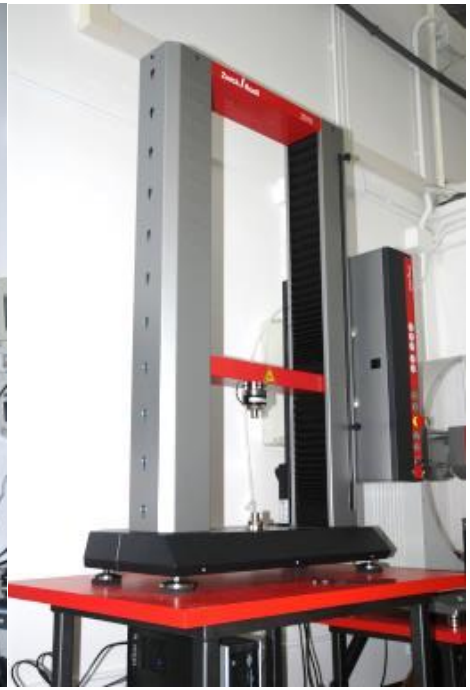

Max load 10KN

Max load 0.5KN

Charpy Pendulum

Biological soft tissues

Have a structure resembling that of rubber:

Long molecular chains which can take a lot of **configurations** of **equal energy**

- Structure indistinguishable from the liquid state in unloaded condition
- Behaviour as elastic solid when pulling force is applied

Entropic elasticity

Hyperelasticity of biological tissues

Hyperelasticity of biological tissues

General constitutive laws

Richter theorem of representation for isotropic materials

$$\boldsymbol{T} = \alpha\, \boldsymbol{I} + \beta\, \boldsymbol{\varepsilon} + \gamma\, \boldsymbol{\varepsilon}^2$$

Strain invariants

$I_1 = \mathrm{tr}(\boldsymbol{\varepsilon})$, $I_2 = ½ \{I_1^2 - \mathrm{tr}(\boldsymbol{\varepsilon}^2)\}$, $I_3 = \det(\boldsymbol{\varepsilon})$

$$\alpha = \frac{\partial F}{\partial I_1} + I_1 \frac{\partial F}{\partial I_2} + I_2 \frac{\partial F}{\partial I_3}$$

$$\beta = \left(\frac{\partial F}{\partial I_2} + I_1 \frac{\partial F}{\partial I_3} \right)$$

$$\gamma = \frac{\partial F}{\partial I_3}$$

Hyperelasticity of biological tissues
Phenomenological models

1. **Neo-Hookean (1 invariant, 1 parameter)**

   $F = \mu/2\ (I_1 - 3)$

2. **Mooney-Rivlin (2 invariants, 2 parameters)**
3. **Generalized Mooney-Rivlin (2 invariants, *n* parameters)**
4. **Ogden (*n* non-fundamental invariants, 2*n* parameters)**
5. **Logarithmic strain (1 invariant, 2 parameters)** $(\varepsilon = ln(\boldsymbol{U})\ )$

   On account of incompressibility

   $I_1 = \mathrm{tr}(\boldsymbol{\varepsilon}) = \ln(J) = 0 \quad I_2 = -\tfrac{1}{2}\,\mathrm{tr}(\boldsymbol{\varepsilon}^2)$

   $F = 2\mu/q\ \exp(-q\ I_2)$ $\quad \boldsymbol{\sigma = 3\mu\ \exp\ (-qI_2)\ \ln(\lambda)}$ $\quad E = 3\mu$

Hyperelasticity of biological tissues
Physical models

1. Independent freely jointed chains

(gaussian model: 1 invariant, 1 parameter)

$$F = 3/2\ kTn_c\ I_1 + F_0$$

The gaussian chain model is equivalent to the neo-hookean model with $\mu = 3\ kTn_c$

2. Arruda-Boyce

(non-gaussian chain network: 1 invariant, 2 parameters)

$$F = \mu\left\{\frac{1}{2}\left(I_1 - 3\right) + \frac{1}{20\lambda_\infty^2}\left(I_1^2 - 9\right) + \frac{11}{1050\lambda_\infty^4}\left(I_1^3 - 27\right) + \ldots\right\}$$

Hyperelasticity of biological tissues

All incompressible models in uniaxial stress

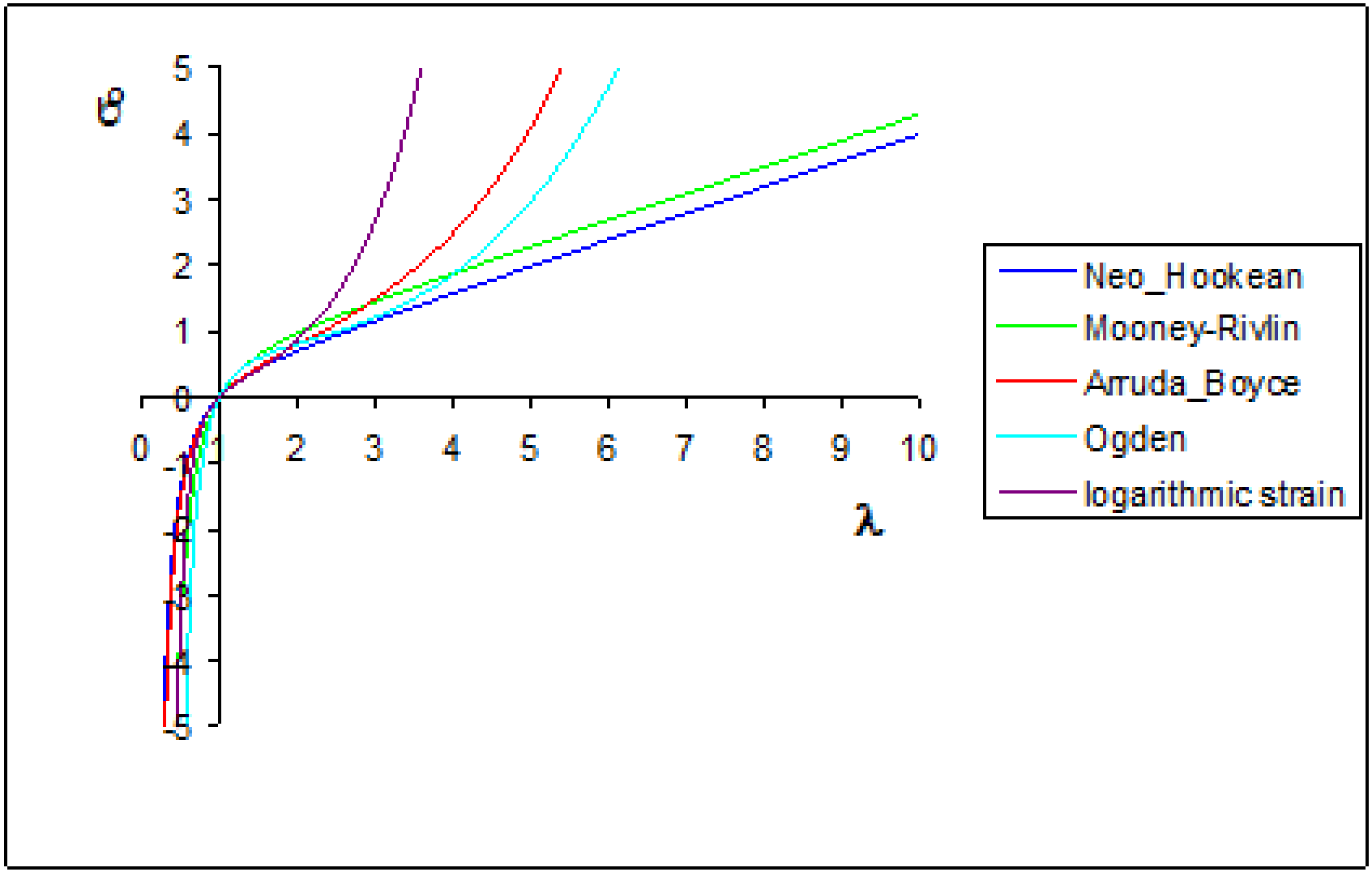

Hyperelasticity of biological tissues
Logarithmic strain model

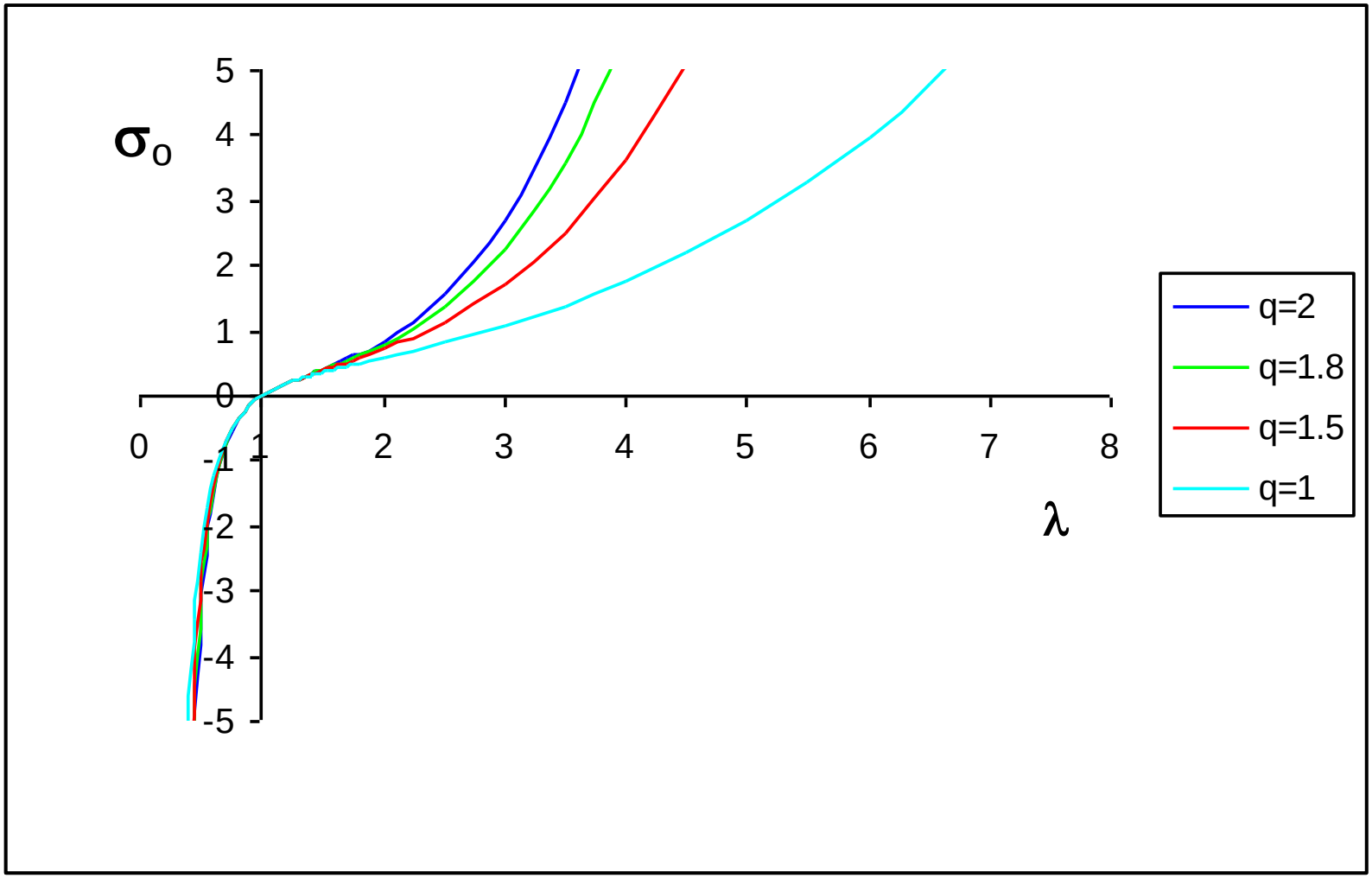

Biological tissues
Vascular system

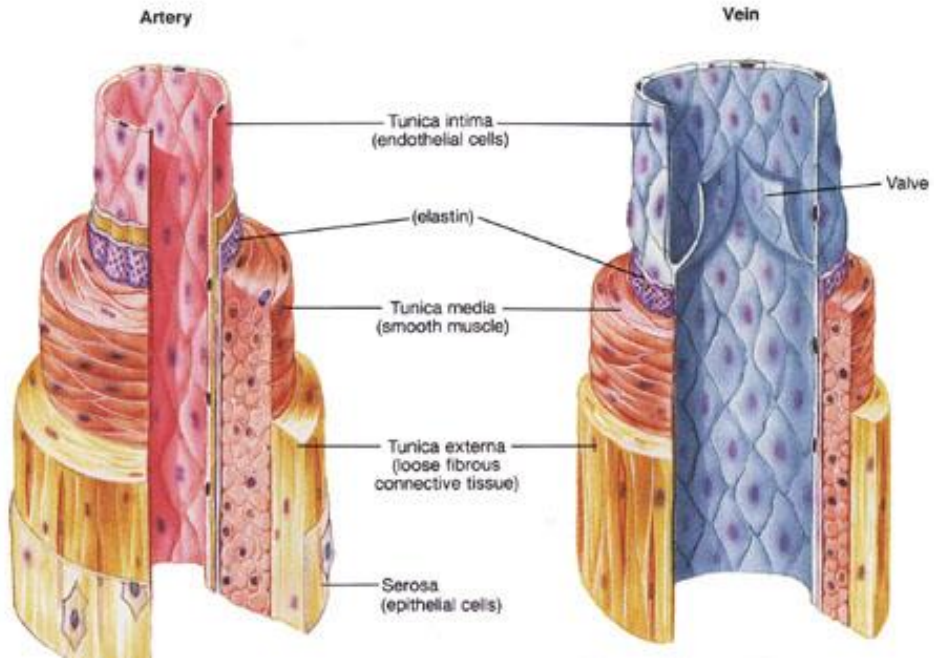

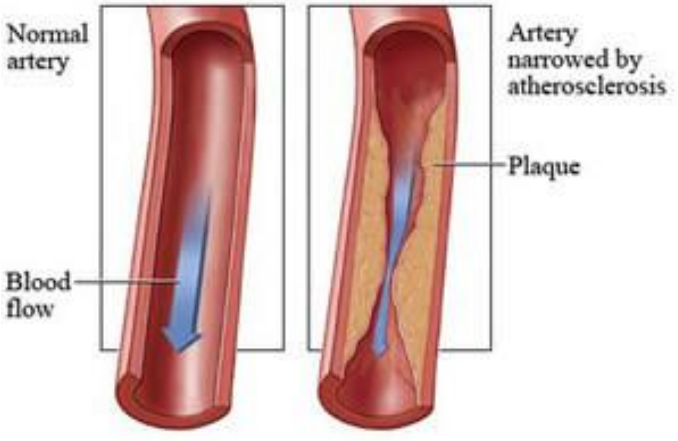

Patologies

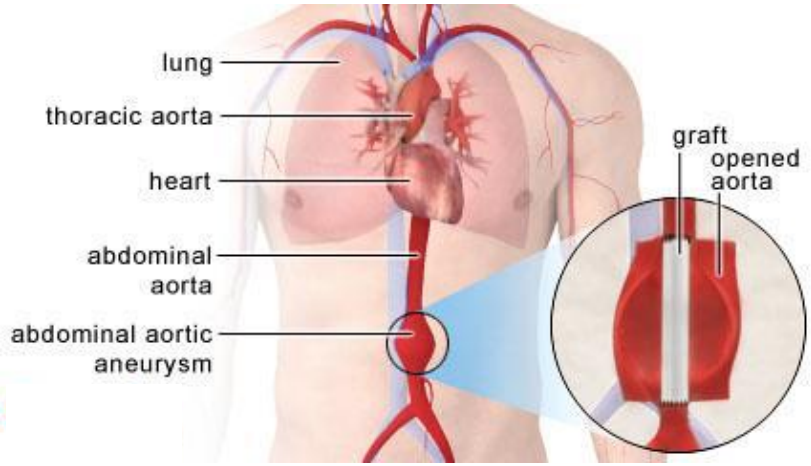

Mechanical analysis of porcine Aorta

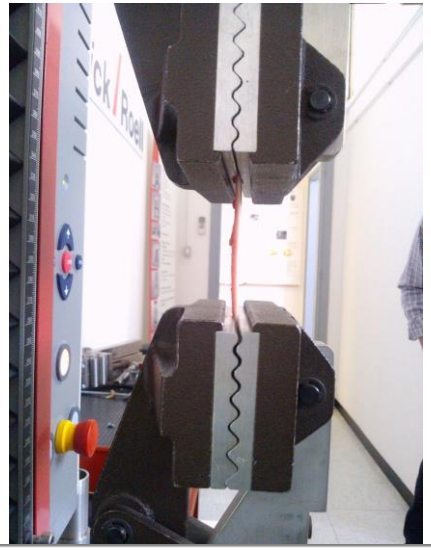

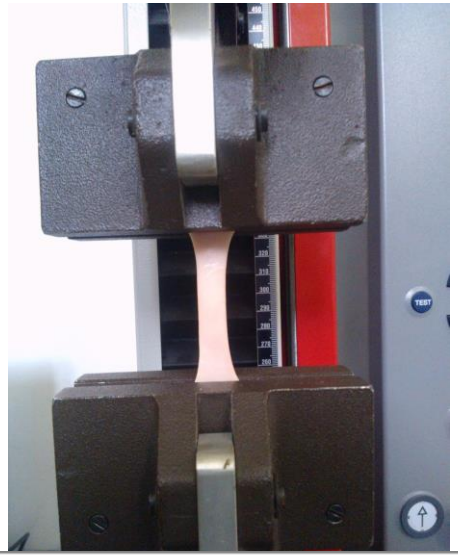

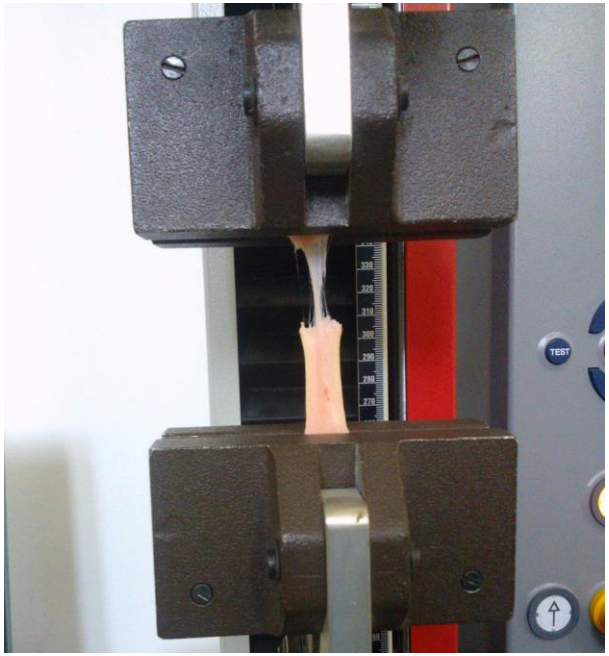

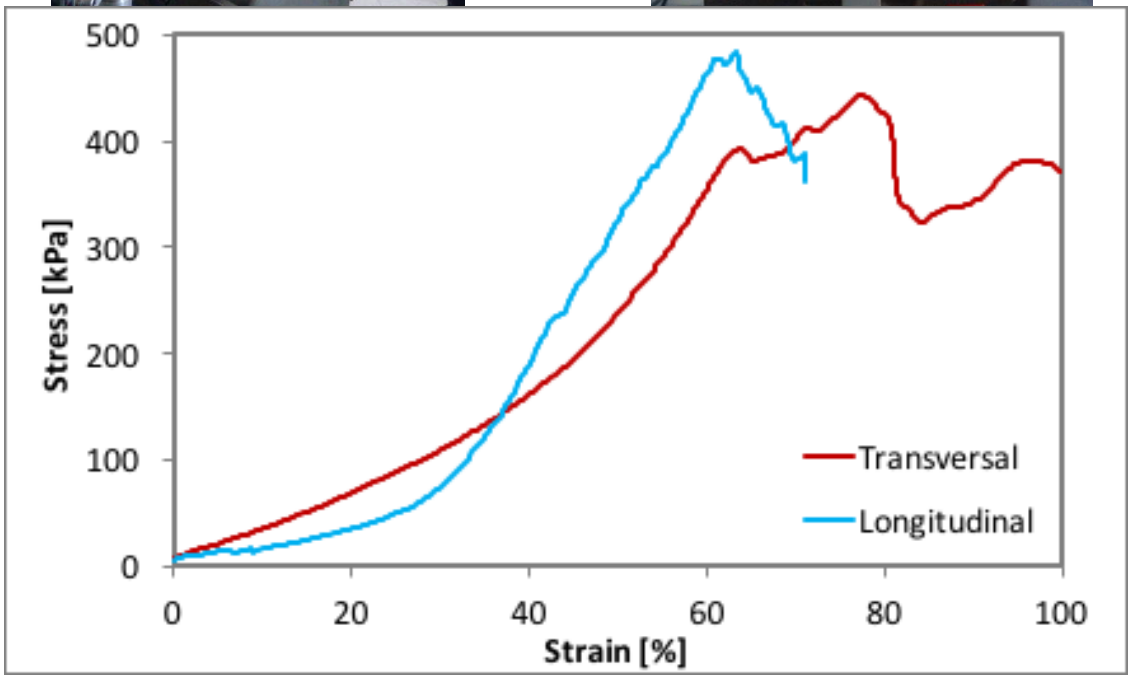

Vascular Electrospun PCL Prosthesis

Prof. P. Perego (DICCA – University of Genoa)

Prof. D. Palombo (Medicine Faculty – University of Genoa)

Vascular prosthesis
Electrospun scaffold

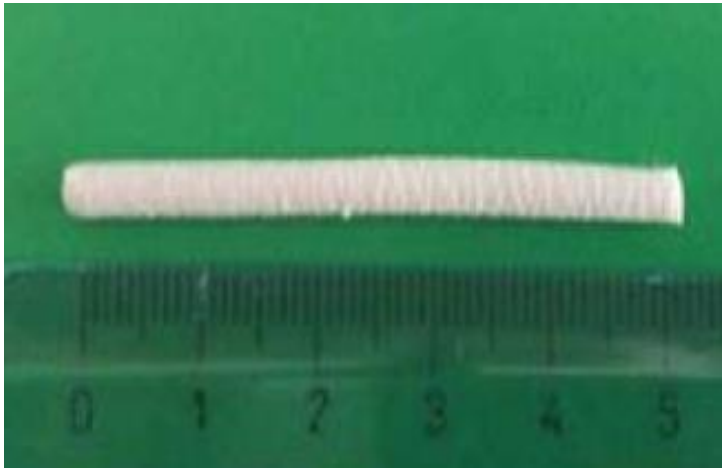

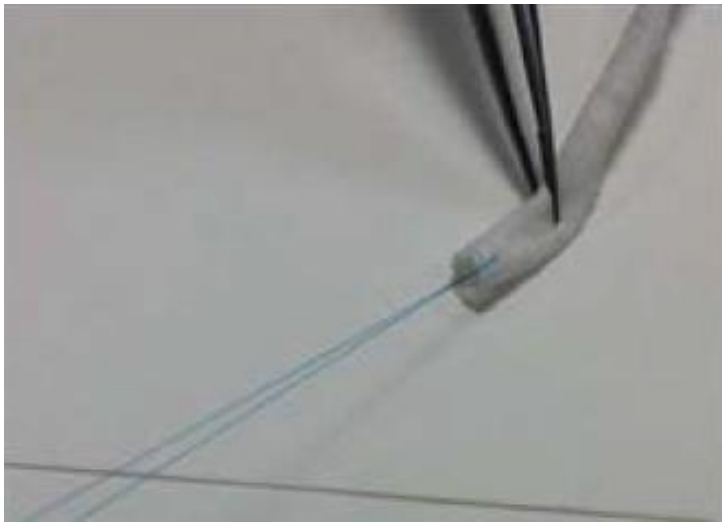

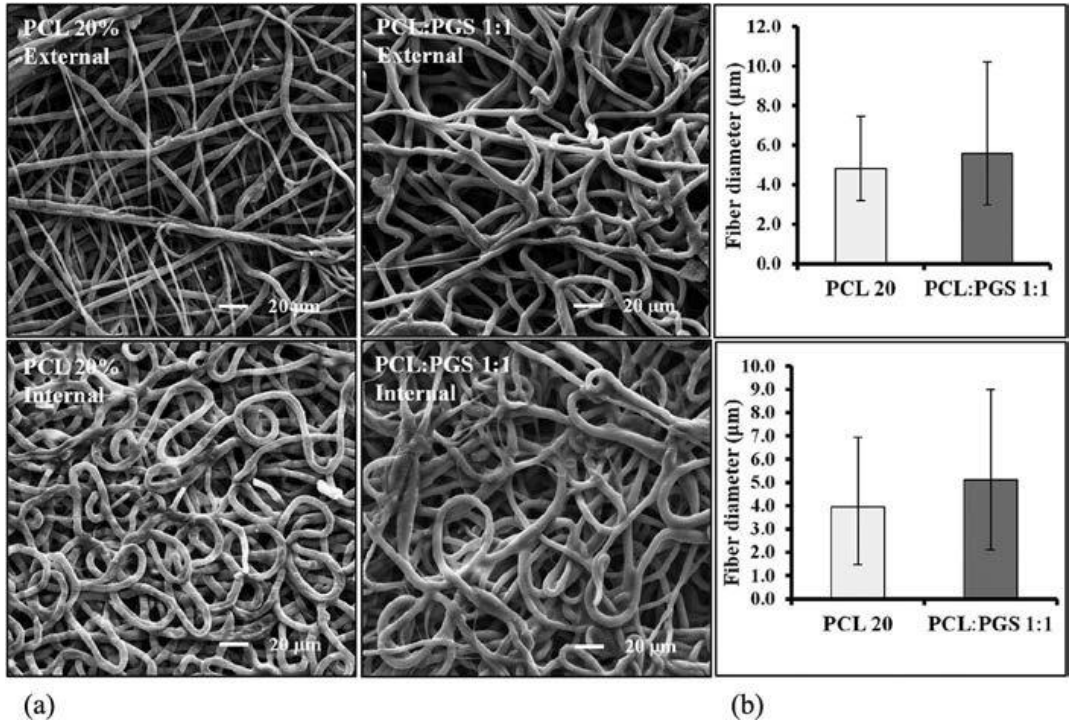

P. Ferrari, B. Aliakbarian, A. Lagazzo et al. Tailored electrospun small-diameter graft for vascular prosthesis *Int J Polym Mat and Polym Biomat* (2016), 66 (12) 635-643 DOI: 10.1080/00914037.2016.1252361

Vascular prosthesis

Tensile mechanical test & Suture retention

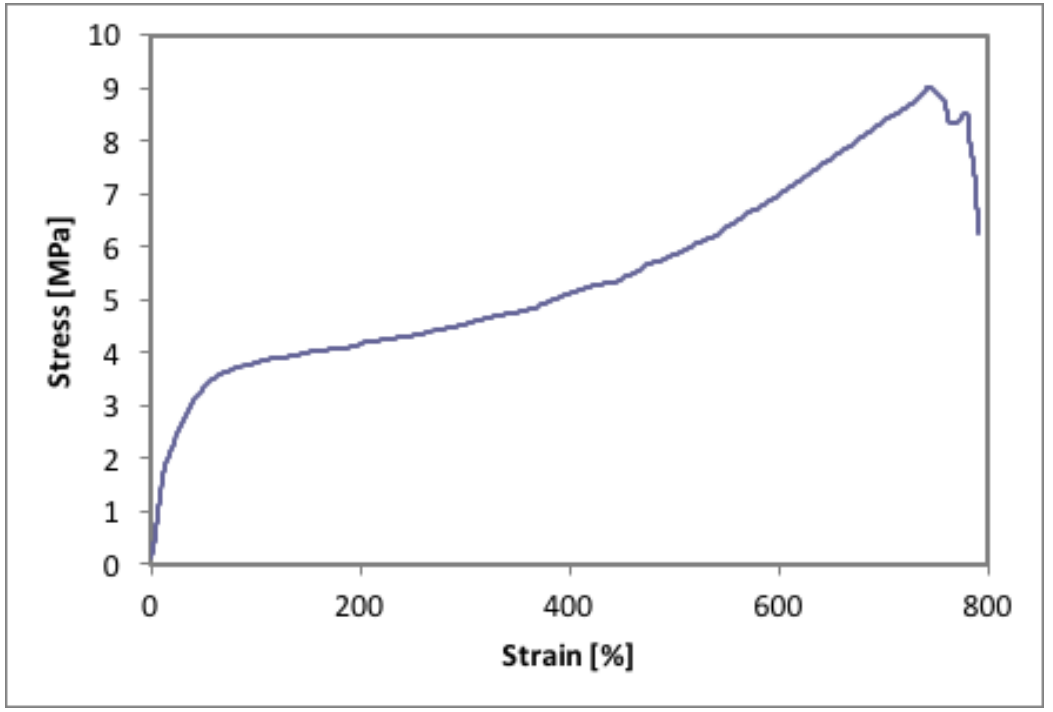

Sample	Young's modulus (MPa)	Tensile strength (MPa)	Elongation (%)	Normalized suture retention (grams-force/mm)
PCL 10%	2.48 ± 0.19^{b}	1.16 ± 0.24^{a}	84.16 ± 7.95^{b}	0.42 ± 0.18^{a}
PCL 15%	4.25 ± 0.22^{a}	1.84 ± 0.75^{a}	282.76 ± 127.72^{a}	6.80 ± 4.17^{a}
PCL 20%	$3.87 \pm 0.36^{a,c}$	$2.37 \pm 0.60^{a,b}$	643.30 ± 30.68^{d}	5.75 ± 2.31^{a}
PCL:PGS 3:1	4.25 ± 0.21^{a}	1.78 ± 0.31^{a}	453.11 ± 19.38^{c}	4.94 ± 1.20^{a}
PCL:PGS 2:1	5.39 ± 0.84^{d}	$1.89 \pm 0.45^{a,b}$	242.83 ± 39.38^{a}	5.98 ± 2.45^{a}
PCL:PGS 1:1	7.61 ± 0.92^{e}	3.14 ± 1.47^{b}	218.48 ± 27.72^{a}	3.84 ± 2.72^{a}
Native human artery	$2.58 \pm 0.34^{b,c}$	1.13 ± 0.06^{a}	46.54 ± 11.32^{b}	4.09 ± 2.12^{a}

Poroelastic biological tissues

Elasticity of foam-like materials

Compressible materials

1. Changing the first two invariants of Cauchy-Green strain

$$I_1^* = I_1 J^{2/3}; \qquad I_2^* = I_2 J^{4/3}$$

2. Addition of a volumetric term $\frac{1}{2} K (J-1)^2$ to the free energy

Neo-Hookean $$F = \frac{\mu}{2} (I_1^* - 3) + \frac{K}{2} (J - 1)^2$$

Model of Blatz and Ko

$$F = \frac{\mu}{2}\left\{\frac{I_2}{I_3} - \frac{1+\nu}{\nu} + \frac{1-2\nu}{\nu} I_3^{\frac{\nu}{1-2\nu}}\right\} \quad \text{for } \nu = 0.25 \quad F = \frac{\mu}{2}\left\{\frac{I_2}{I_3} + 2I_3^{1/2} - 5\right\}$$

Elasticity of foam-like materials

Compressible materials: logarithmic strain model

$$I_1 = \ln(J)$$

$$F = \frac{2\mu}{q} \exp(s\, I_1^2 - q\, I_2)$$

where $s = \frac{1-\nu}{2(1-2\nu)}\, q$

Constitutive eq. for F

$$\boldsymbol{T}^{(R)} = \frac{\nu}{1-2\nu} qFI_1\, \boldsymbol{I} + qF\, \boldsymbol{\varepsilon}$$

$$p = B \ln(J) \exp\left(q \frac{1+\nu}{6(1-2\nu)} \ln^2(J) \right)$$

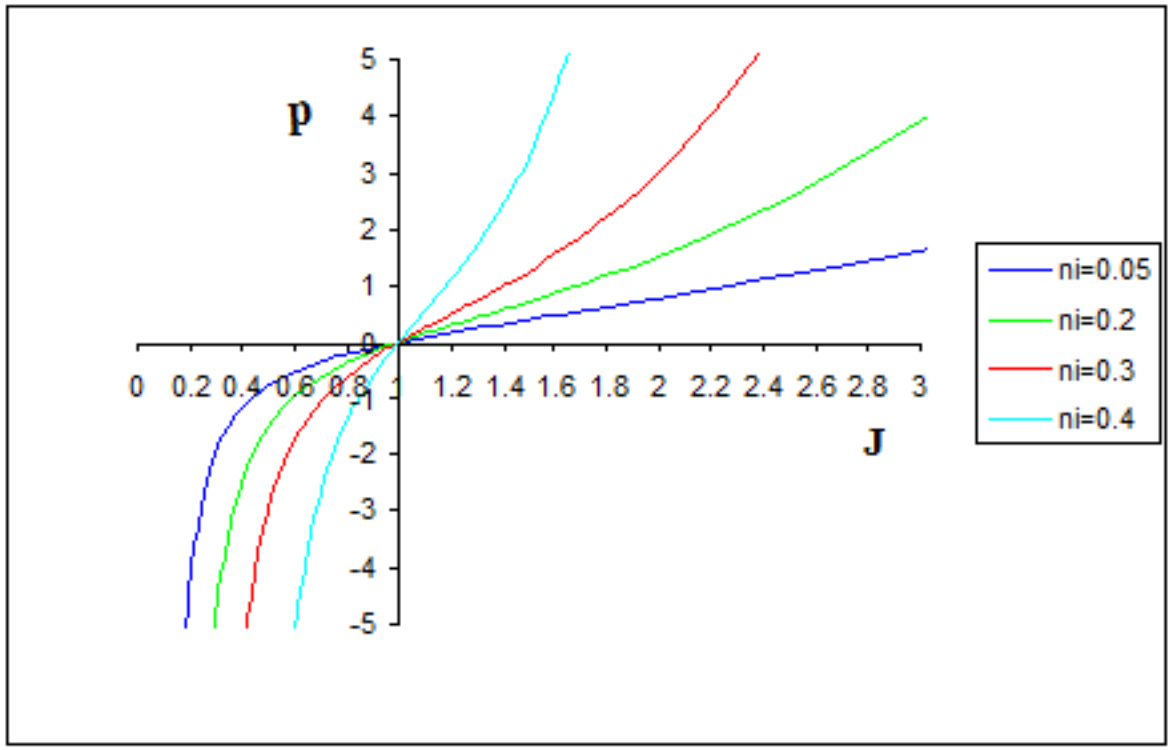

Poroelastic materials

The system is **biphasic**:

- one phase is the incompressible fluid
- the other is the porous matrix or **skeleton**.

The fluid is assumed to saturate the porosity of the skeleton.

The skeleton

hyperelastic (compressible or incompressible)

structures:

- aggregate of particles (soldered at their contact points or even loose like sand)
- foam (an array of cells or spherical voids communicating through openings or channels in their walls)
- sponge (a 3-d network of relatively slender elements or trabeculae like the structure of cancellous bone)
- vascolarized tissue (fractal features).

Poroelastic materials

drained condition

the liquid can freely flow through the pores (negligible effect of viscosity).

Empty skeleton.

undrained condition

the outlet of the fluid is partially or totally inhibited

external surface is waterproof

pore channels very small

perfused medium

the fluid enters the medium at a given pressure and gets out from surface openings at a rate which depends:

viscosity

pore structure (porosity, pore diameter and length, tortuosity)

- perfusing fluid causes an increase of porosity
- skeleton micromechanically incompressible

$$J = \frac{1 - f_o}{1 - f}$$

Poroelastic materials

Ashby's models

fundamental cubic structures

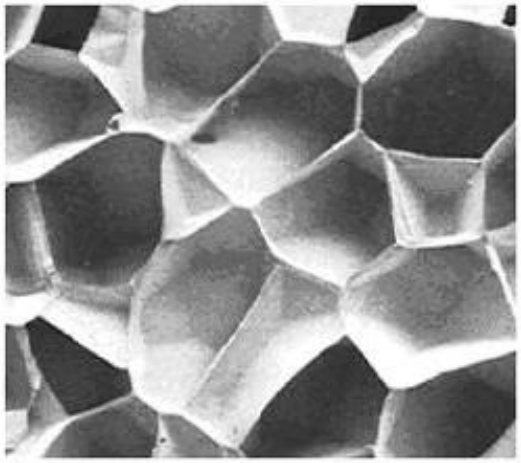

- **cellular-solid** prototype:
  matter distributed on the cube faces
  (*t* is the wall thickness, openings are not considered)

$$\rho = 1 - (1 - t/a)^3$$

- schematic **spongeous** solid:
  matter distributed along the cube edges
  in the shape of rods, each with length *a*
  and square cross-section of size *t*

$$\rho = 3t^2/a^2 - 2(t/a)^3$$

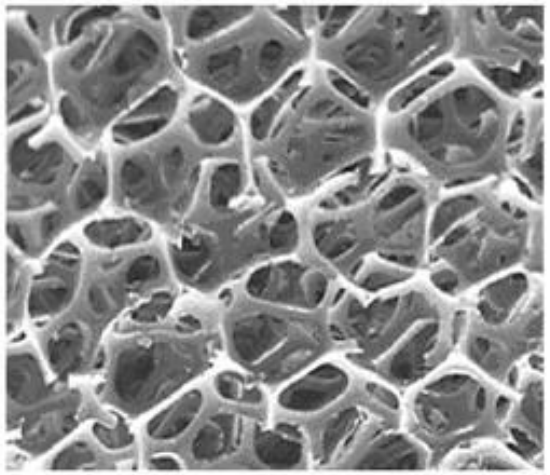

Poroelastic materials

Ashby's models: axial loading (no buckling)

$$\varepsilon = \frac{\sigma a^2}{EA} \Rightarrow E^* = EA/a^2$$

- *Cellular structure*

$$A/a^2 = 2t/a - (t/a)^2 = 1-(1-t/a)^2 \qquad \frac{E^*}{E} = 1 - f^{2/3}$$

- *Spongeous structure*

$$A/a^2 = (t/a)^2$$

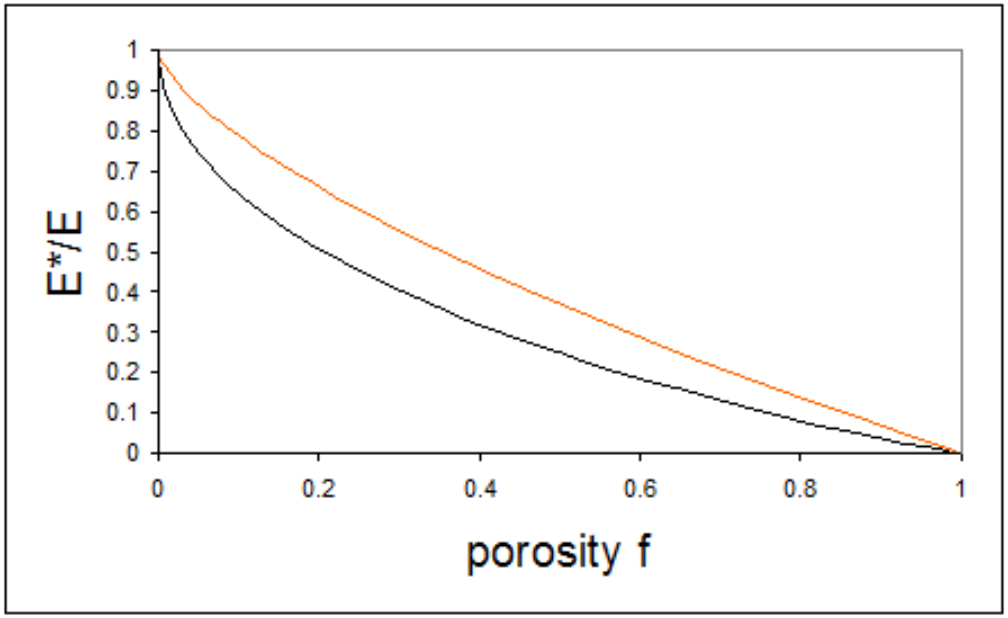

Poroelastic materials

Effect of perfusion pressure

Logarithmic strain model.

p_0 initial perfusion pressure;

f_0 natural porosity of the material in undeformed state

B^* bulk modulus for infinitesimal strain

J_0 volumetric stretch

$$p_0 = B^* \ln(J_0) \exp\left(q \frac{1+\nu}{6(1-2\nu)} \ln^2(J_0) \right)$$

Effect of external load

$$p = B^* \ln(J_L) \exp\left(q \frac{1+\nu}{6(1-2\nu)} \ln^2(J) \right) \exp\left(\frac{q}{2} \mathrm{tr}(\boldsymbol{D}^2) \right)$$

$\boldsymbol{J = J_L J_o}$ **(J_o >1, J_L < 1)**

J_o effect of the perfusion pressure

J_L contribution of the loading.

The material may collapse when J becomes less than the unity (i.e. $J_L < 1/J_o$)

Poroelastic materials

Effect of external load: Uniaxial compression

$\varepsilon = \ln(\lambda)$

$\ln(J_L) = (1-2\nu)\varepsilon$

$\ln(J) = \ln(J_o)+(1-2\nu)\varepsilon$

$$\boldsymbol{D} = \frac{1}{3}\begin{bmatrix} -(1+\nu)\varepsilon & 0 & 0 \\ 0 & -(1+\nu)\varepsilon & 0 \\ 0 & 0 & 2(1+\nu)\varepsilon \end{bmatrix}$$

$$\mathrm{tr}(\boldsymbol{D}^2) = \frac{2}{3}(1+\nu)^2\varepsilon^2$$

$$\sigma = \frac{4\mu^*}{3B^*}(1+\nu)\,\frac{p}{\ln(J_L)}\varepsilon + p$$

$$p = B^*(1-2\nu)\varepsilon\ \exp\left(q\frac{1+\nu}{6(1-2\nu)}\left[\ln(J_o)+(1-2\nu)\varepsilon\right]^2\right)\exp\left(\frac{q}{3}(1+\nu)^2\varepsilon^2\right)$$

Poroelastic materials

uniaxial compression: numerical simulation

Parameters:

Skeleton porosity in the undeformed state: $f_o = 0.14$

Micromechanical moduli: $E_o = 5$ kPa ($\nu_o = 0.45$) , $\mu_o = 1.72$ kPa

Macromechanical moduli: $E^* = E_o (1- f_o)^k$; $\mu^* = \mu_o (1- f_o)^{k'}$:

$k = 2.5$; $k' = 3$; ($\nu = 0.05$) ; $B^* = \frac{E^*}{3(1-2\nu)}$

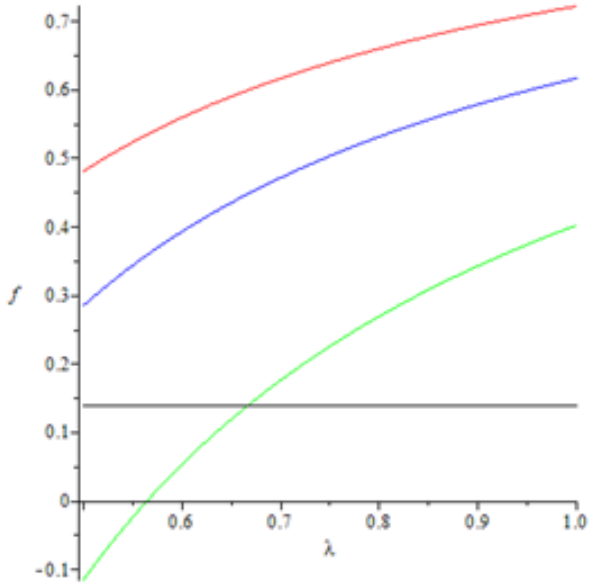

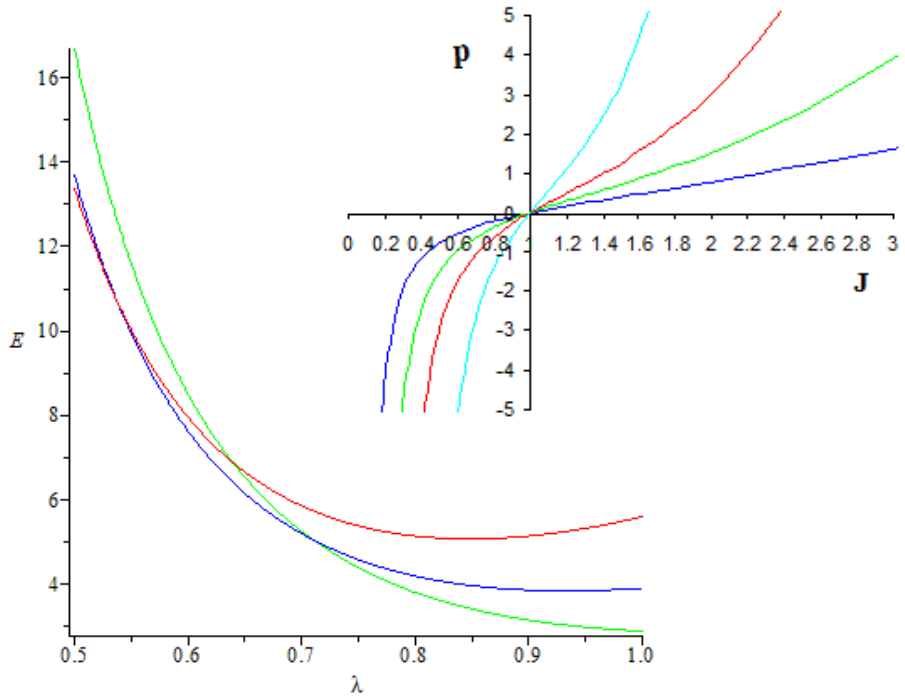

p_0= 0.5 Kpa green, p_0= 1 Kpa blue, P_0 = 3 Kpa red

Biological poroelastic tissues

Hepatic tissue

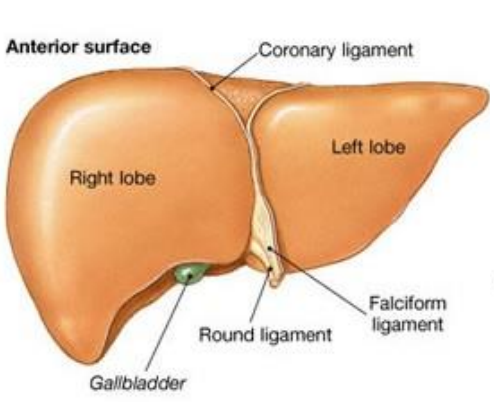

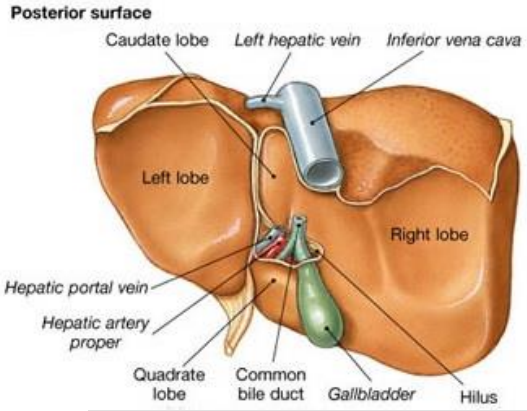

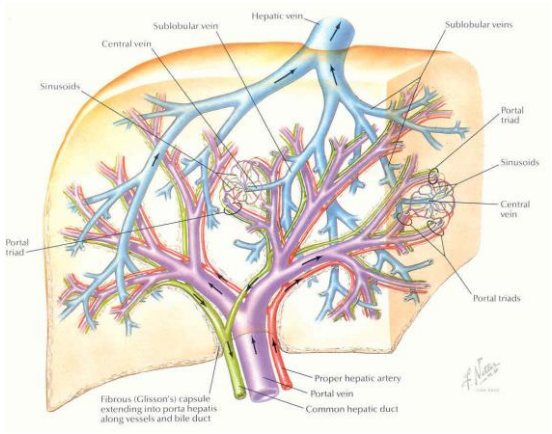

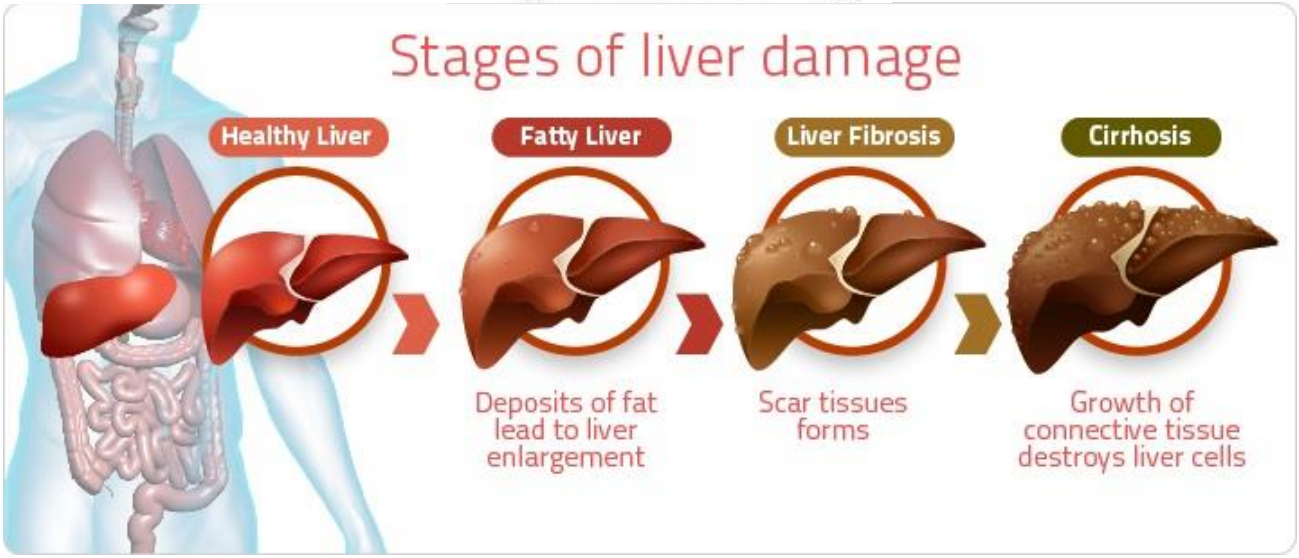

Liver diseases modify the mechanical properties of the liver

Microcirculation deteriorates and Liver tissues fail to receive the proper amount of oxygen

Mechanical characterization of rat liver tissue in perfusion

Perfusion experimental setup

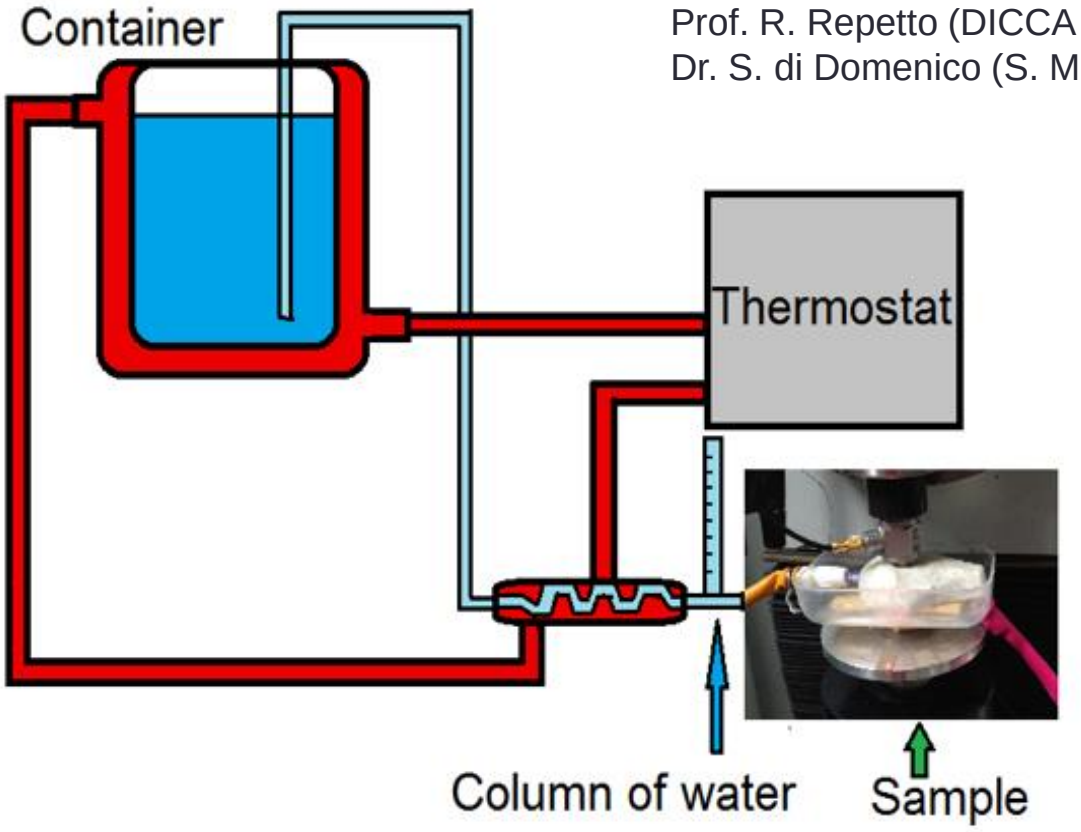

Collaboration with:
Prof. R. Repetto (DICCA – University of Genoa)
Dr. S. di Domenico (S. Martino Hospital - Genova)

Porous matrix Project to simulate rat liver behaviour: Fluidodynamics **PhD** (Ing. V. Baronti)

Mechanical characterization of rat liver tissue in perfusion

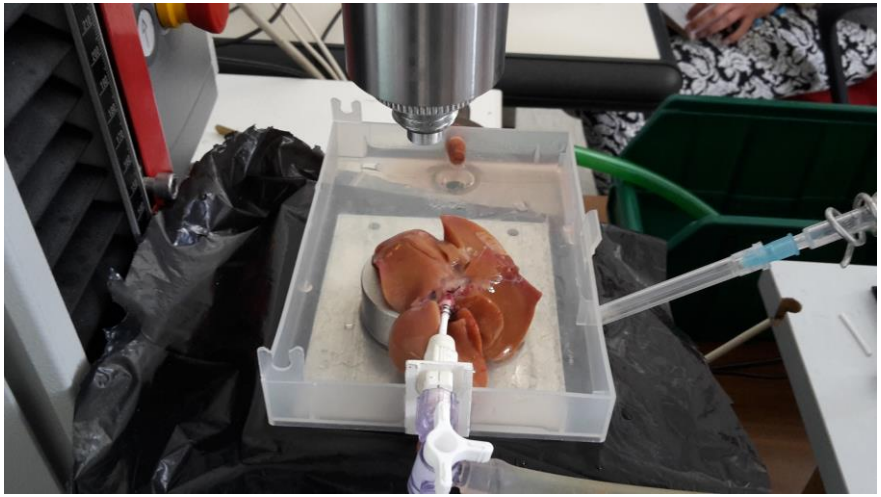

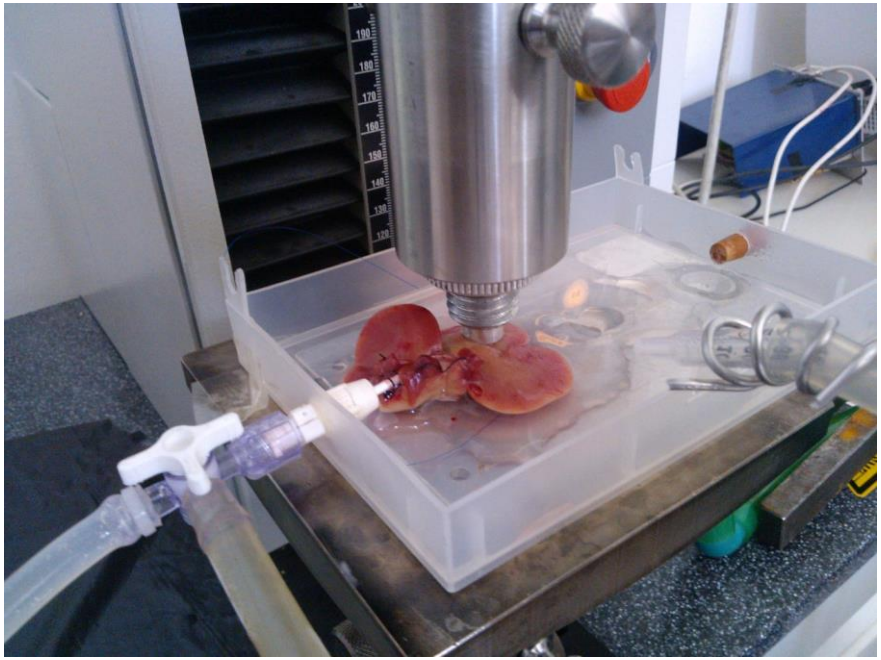

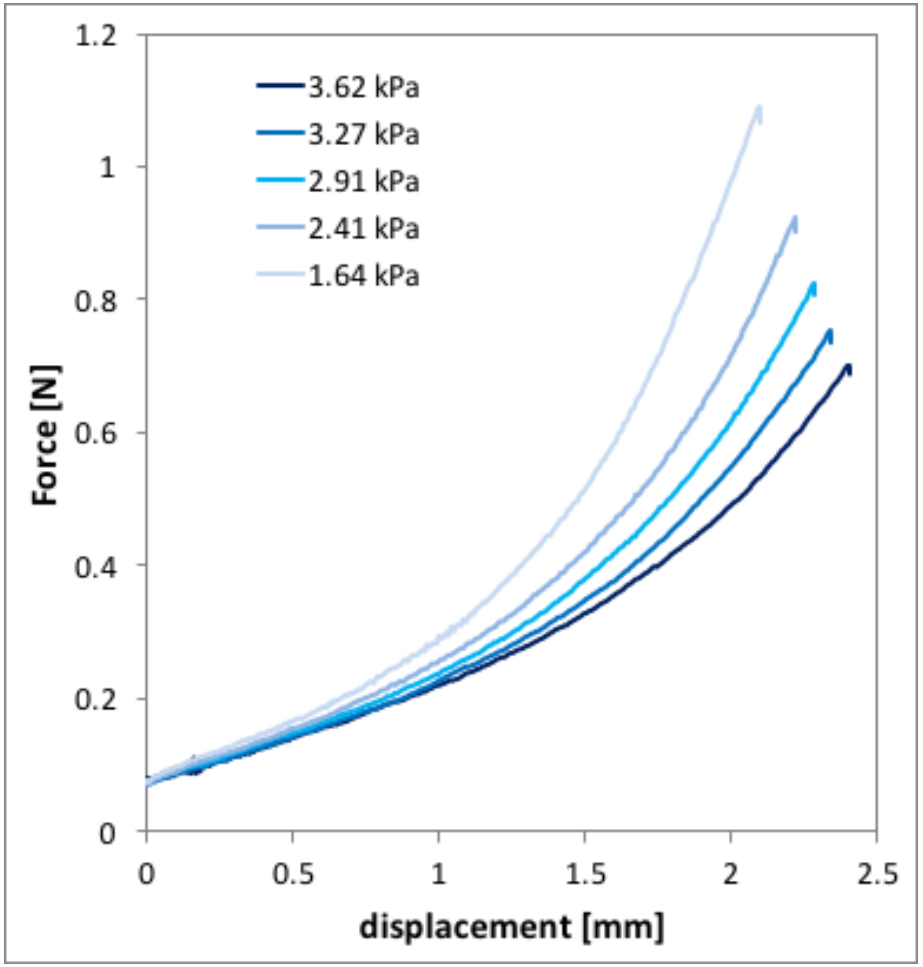

Compressive tests at different flow rate

Mechanical characterization of rat liver tissue in perfusion

Results

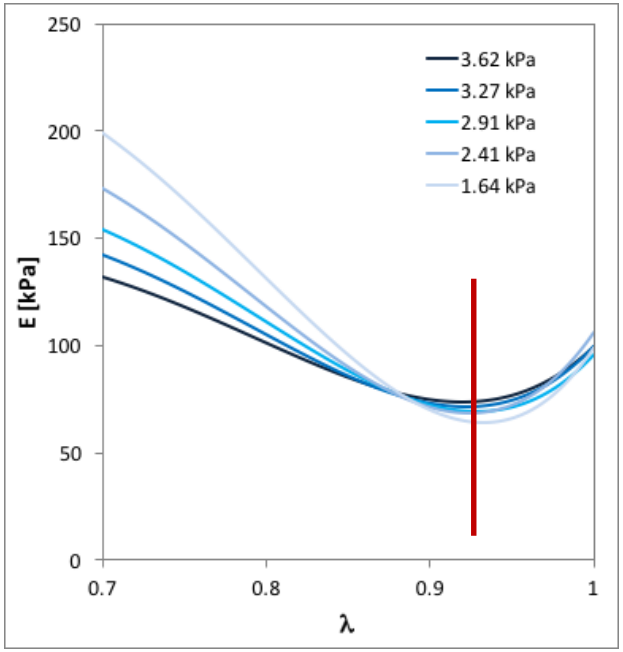

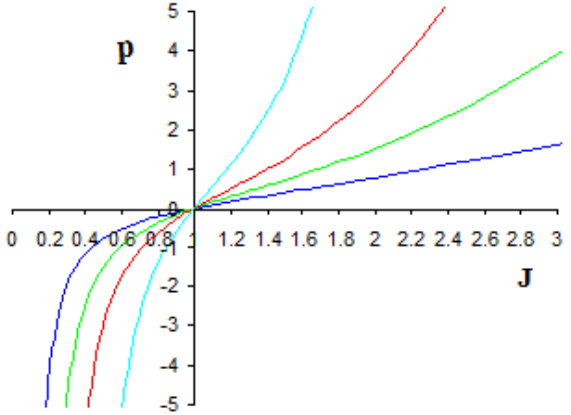

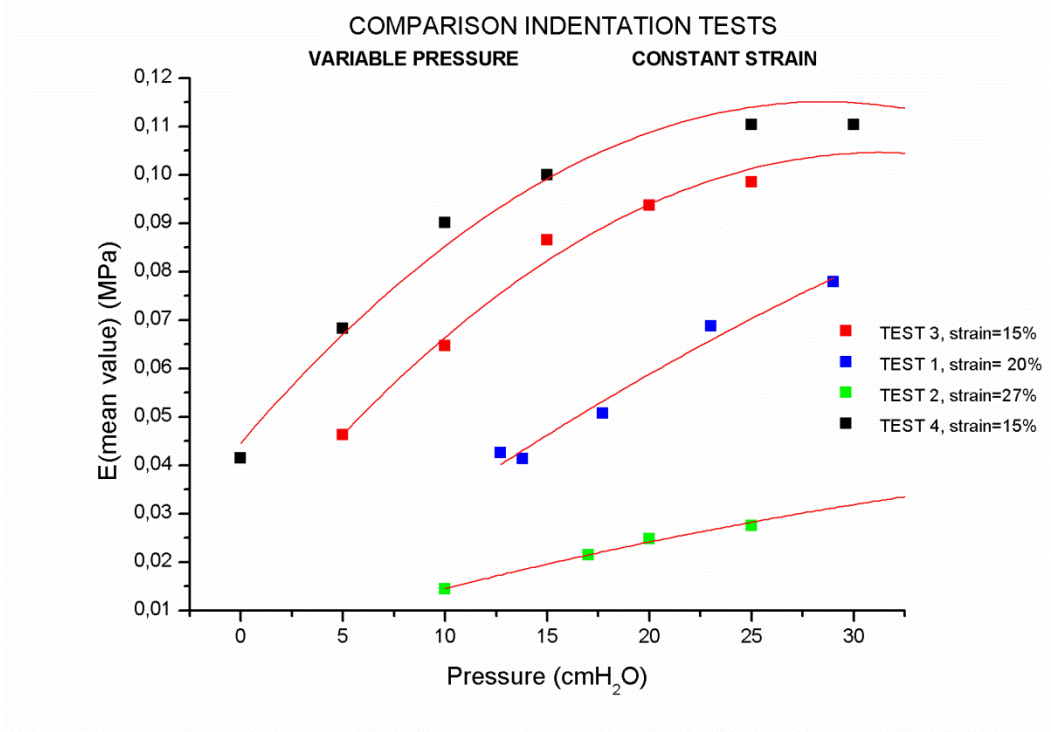

Meniscus

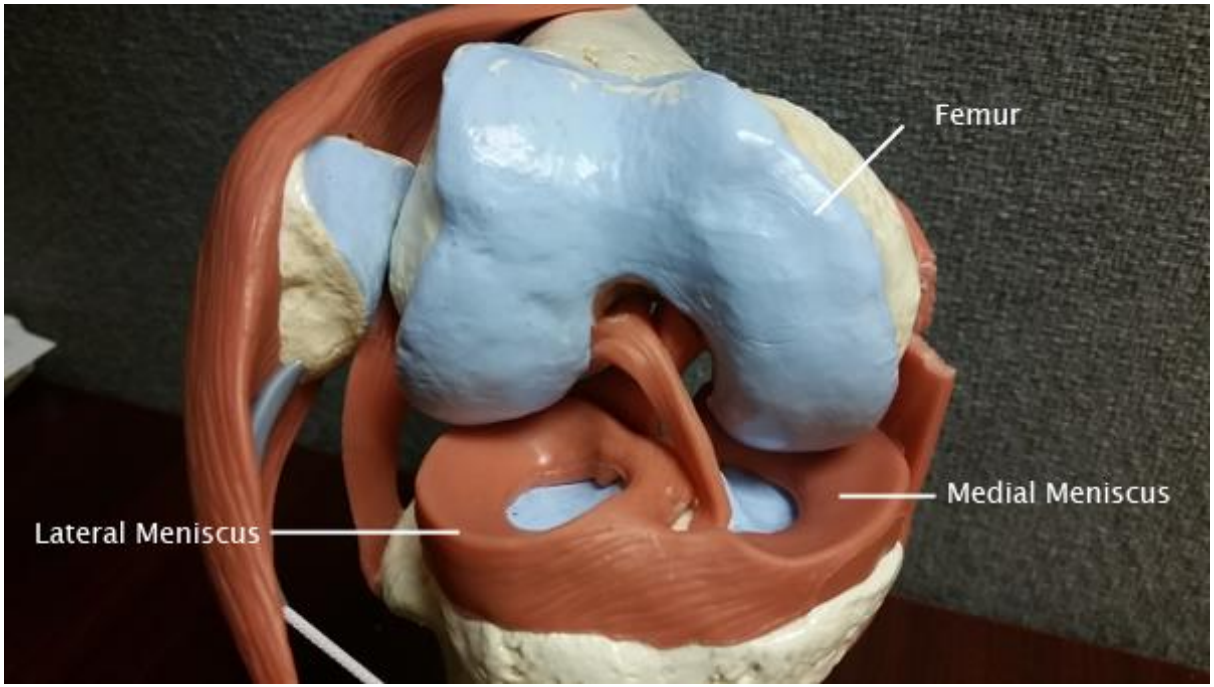

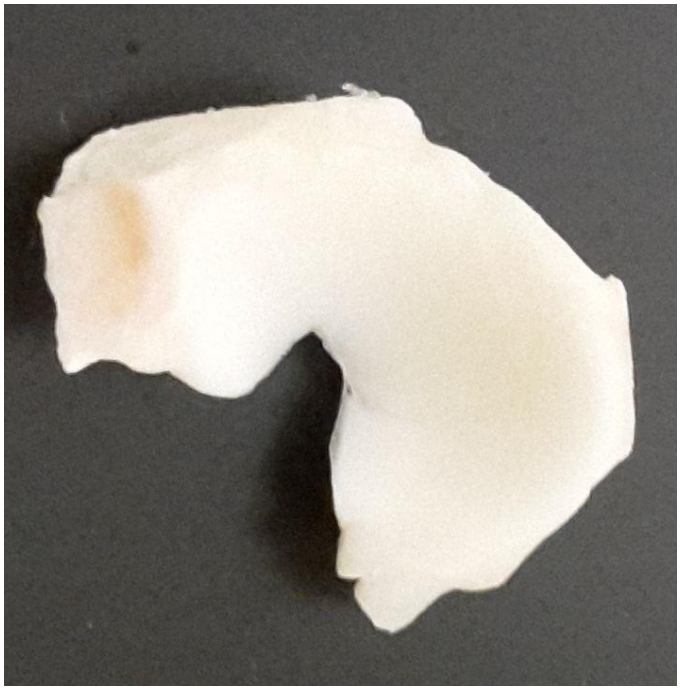

Menisci attenuate, thanks to their elastic compliance, the contact stresses on the condyle surfaces, thereby safeguarding the underlying articular cartilage and preventing osteoarthritis.

Meniscal Tear

Meniscal Tear is a common pathology of the knee that in many cases requires an intervention of meniscectomy, which both in the immediate and in the progress may be the cause of

- impaired joint functionality
- flattening of the condyle
- narrowing of the joint space
- ridge formation
- osteoarthritis.

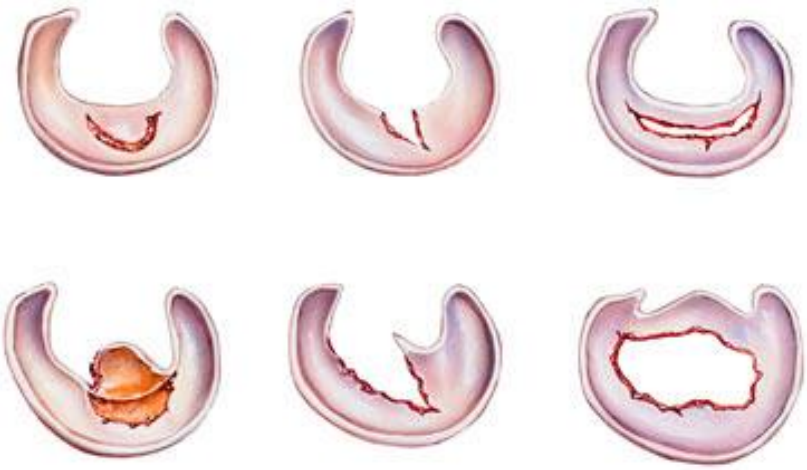

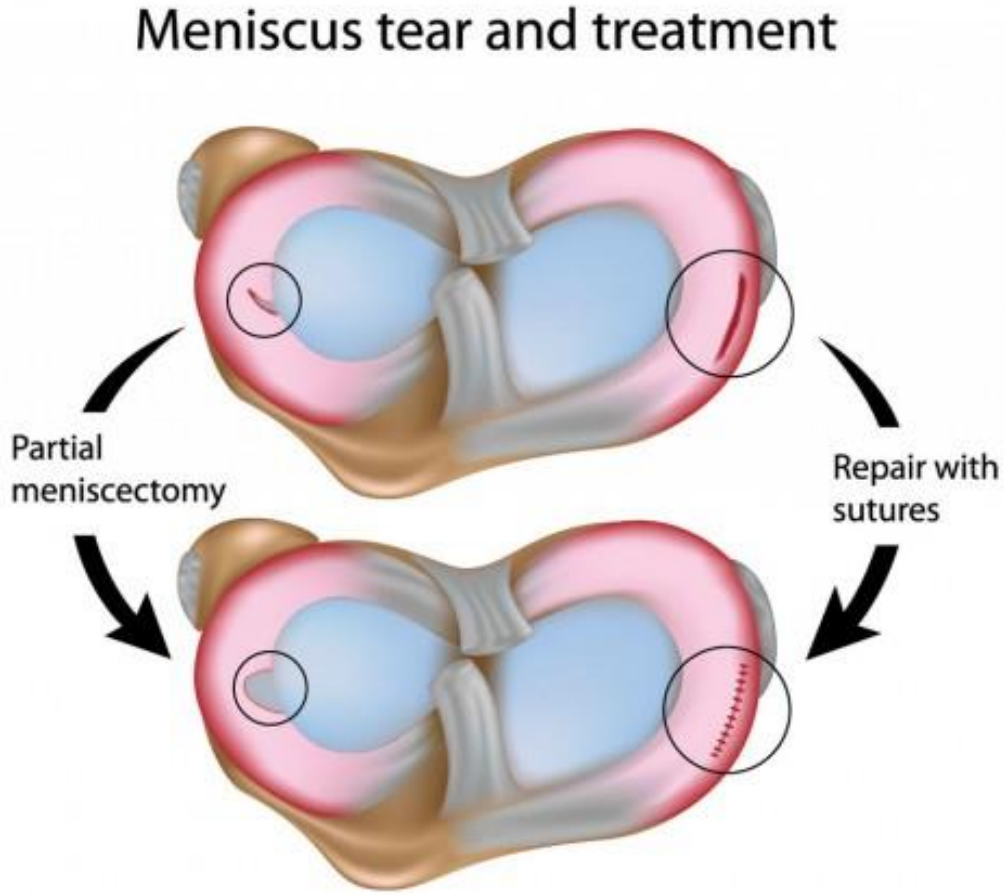

The principles of repair include smoothing and abrading the torn edges and bordering synovium to promote bleeding and healing

S.C. Mordecai, N. Al-Hadithy, H.E. Ware, C.M. Gupte:Treatment of meniscal tears: An evidence based approach, *World J Orthop.* **5**[3](2014)233–241

The use of **cadaveric meniscal allografts** remains the golden standard, but suffers from:

- **penury of donor tissue**
- **risk of infections**
- **size matching**

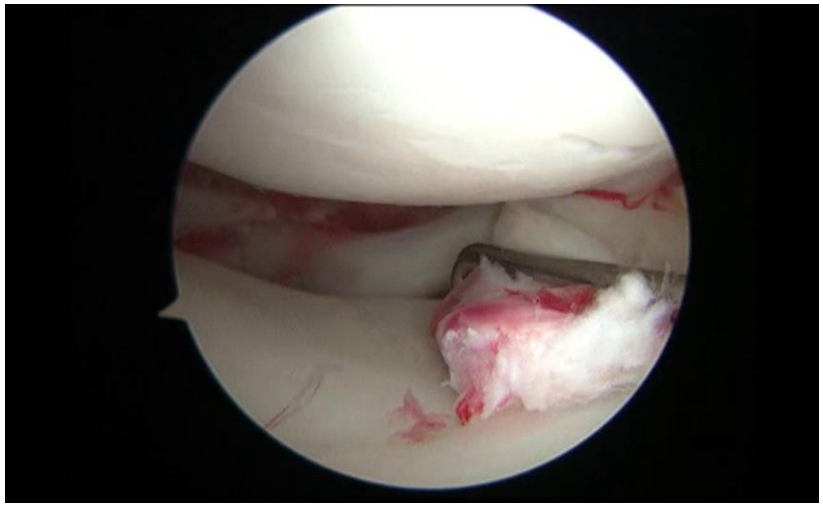

Therefore there is a growing interest in artificial meniscus prostheses

Characterization of meniscus tissue is still to be desired for the development of more effective approaches

[J.J.Ballyns, T.M.Wright, L.J.Bonassar: Effect of media mixing on ECM assembly and mechanical properties of anatomically-shaped tissue engineered meniscus, Biomaterials 31 (2010) 6756-6763]

State of Stress

The state of stress generated by a vertical load (P) in the core of the meniscus does not simply create a compressive stress (σ_{33}) in the load direction, a tensile radial stress (σ_{rr}), but also tangential circumferential hoop stresses ($\sigma_{\theta\theta}$), shear stresses..

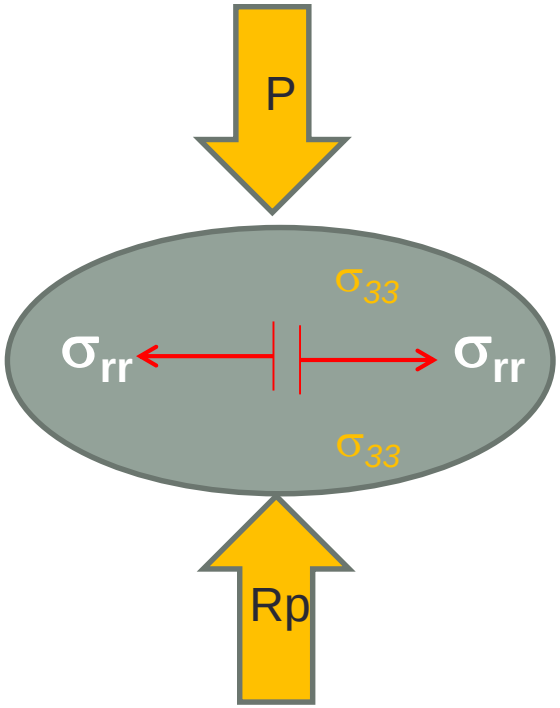

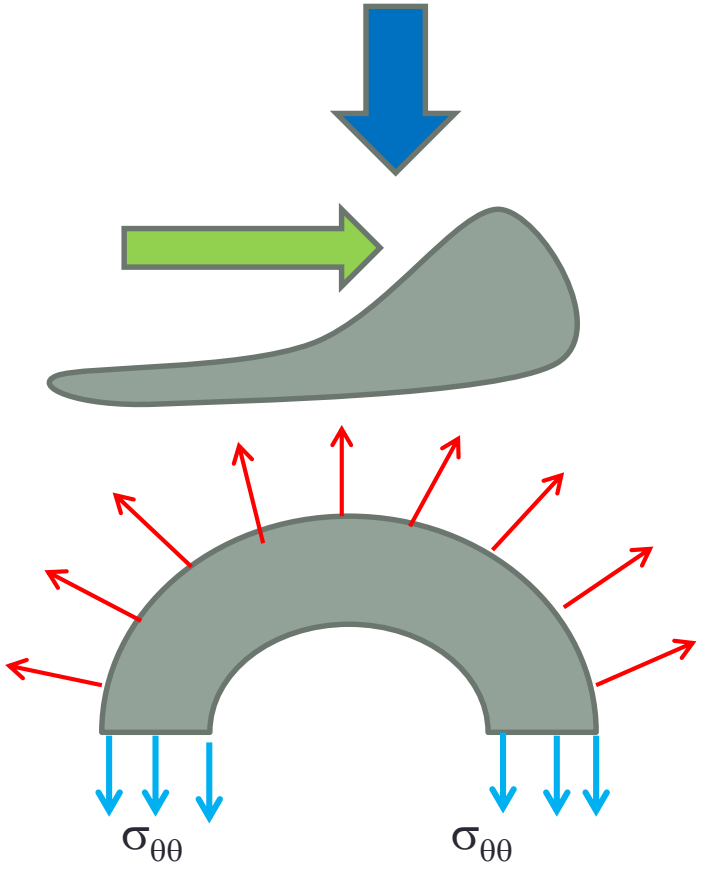

The Storage Temperature

Harvesting and storage of menisci

Deep-freezing at -80 °C or less at a high cooling rate is recommended by several authors for preservation of meniscal allografts and should be considered the golden standard also for the storage of tissue to be used in mechanical testing.

[P. Mickiewicz, M. Binkowski, H. Bursig and Z. Wróbel : Preservation and sterilization methods of the meniscal allografts: literature review. *Cell Tissue Bank* (2014) **15**:307–317 DOI 10.1007/s10561-013-9396-7)]

The Storage Temperature

Non perfect storage conditions: Problems

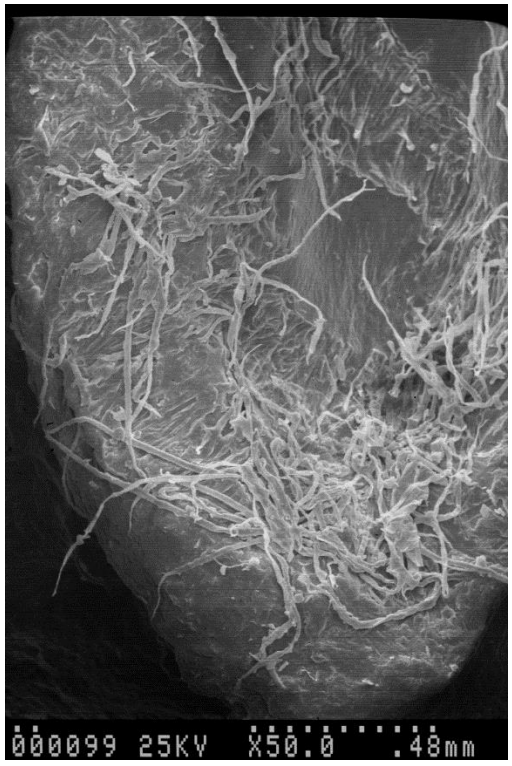

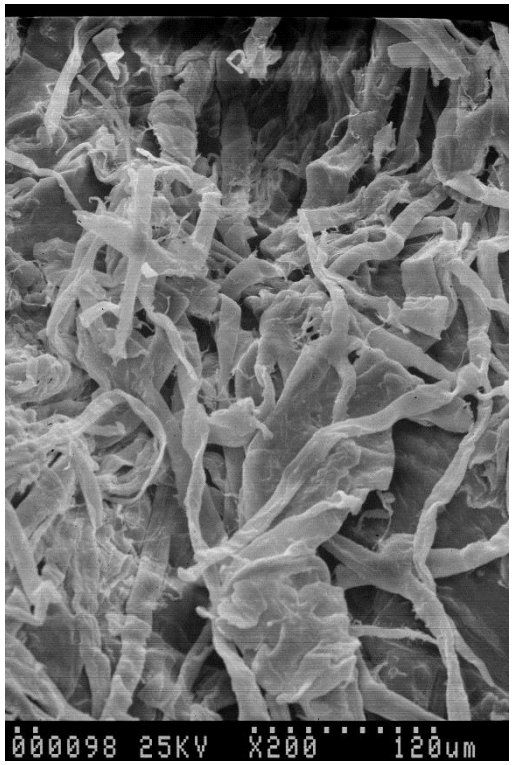

Damage of fibrils

The testing Methods

I - Uniaxial compressive loading

Cylindrical samples (4 mm in diameter) for compression tests from 3 different regions of a meniscus

The cylinder is cut perpendicularly to the tibial plateau, by using a histology punch, and transversally by a sharpened blade to obtain two flat and parallel surfaces

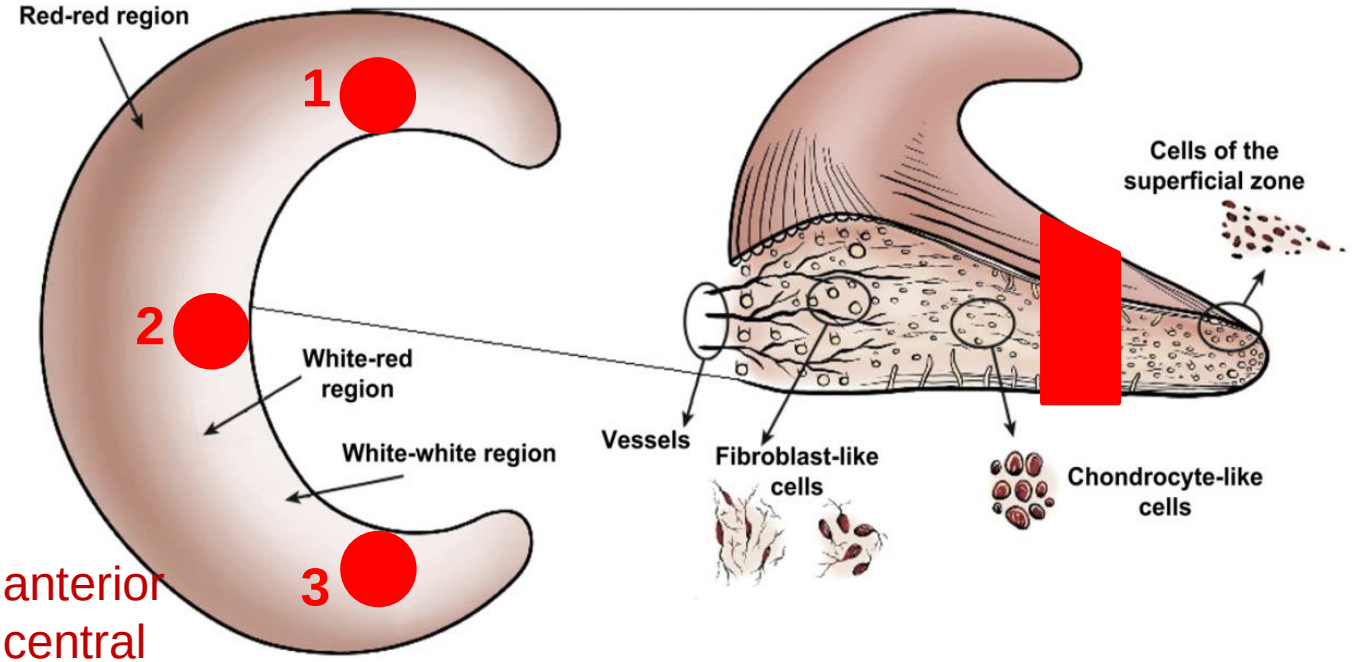

Region 1: anterior
Region 2: central
Region 3: posterior

The testing methods I.

Meniscus sample after thawing and specimen harvesting

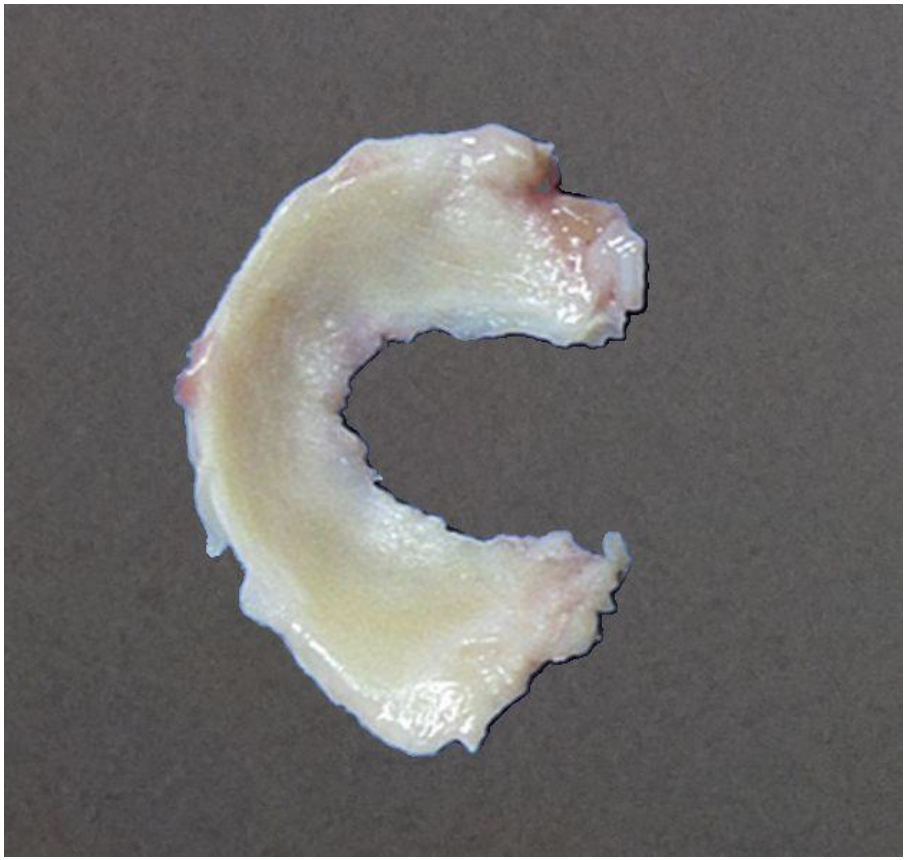

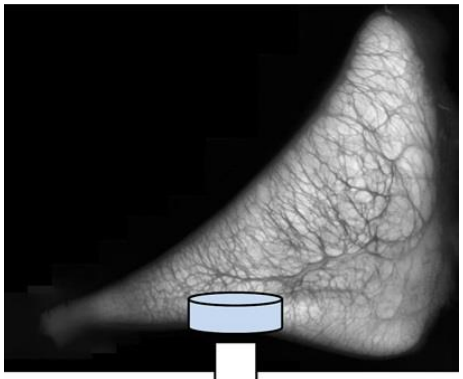

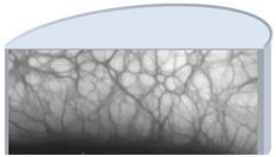

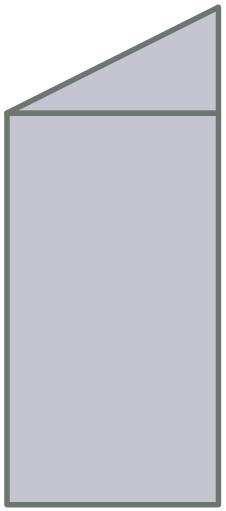

The testing Methods

Static test (5 mm/min). Behaviour of sample in partial swelling.

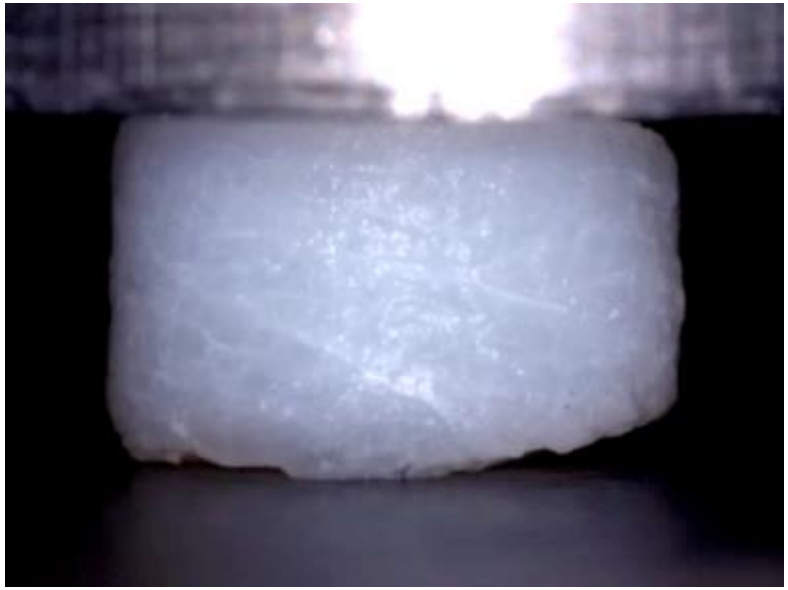

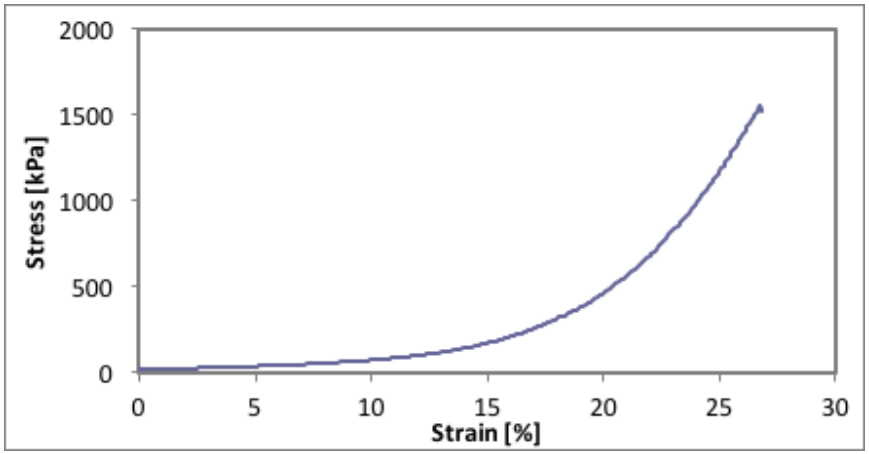

Standard solid model

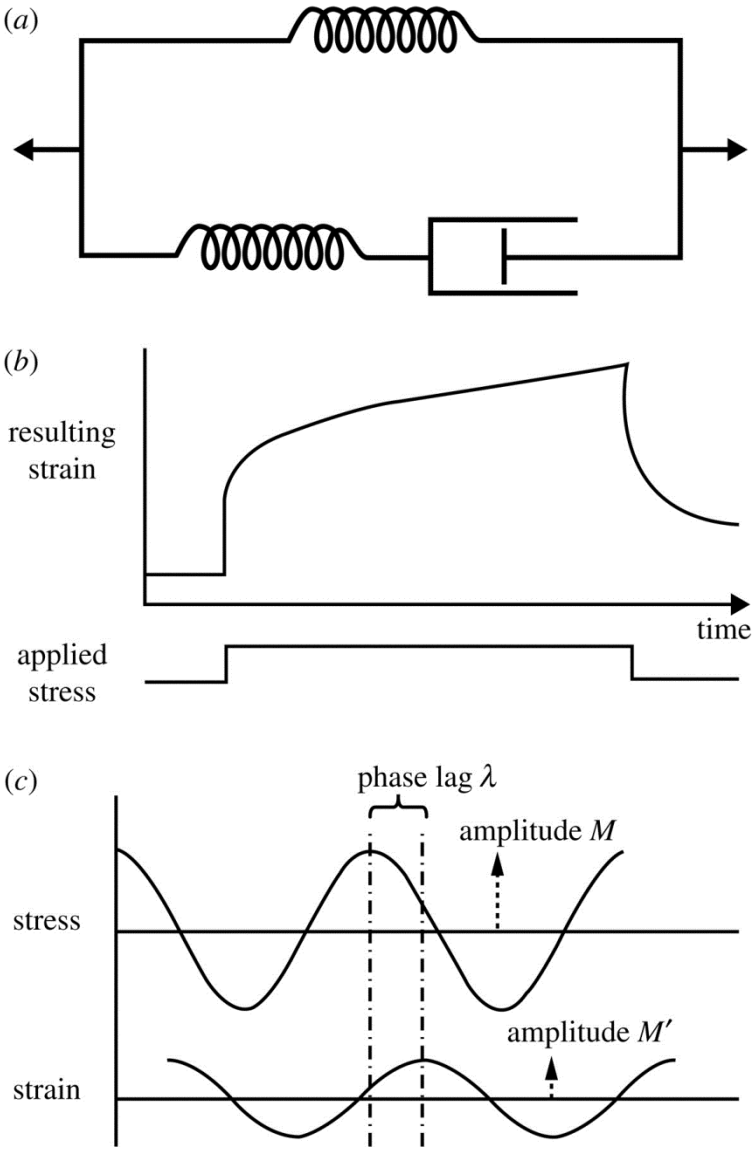

DMA analysis

- Dynamic mechanical properties refer to the response of a material as it is subjected to a periodic force.

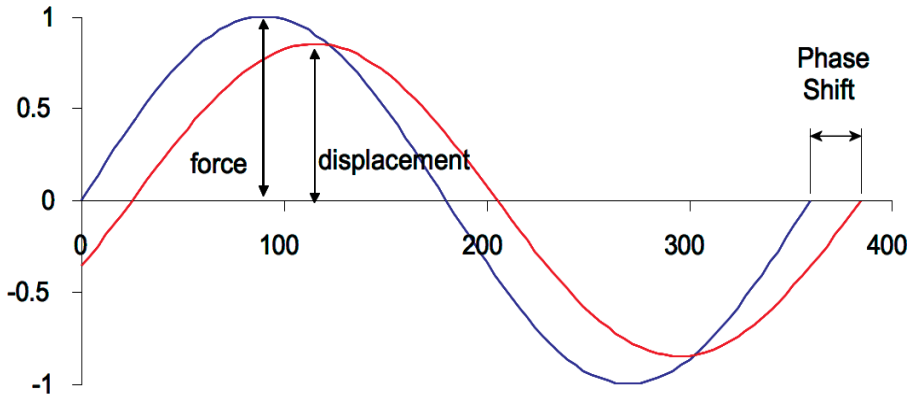

- $\sigma(t) = \int_{-\infty}^{t} \Phi(t-\tau)\varepsilon(\tau)d\tau$
- $\hat{\sigma}(\omega) = \hat{\Phi}(\omega) \cdot \hat{\varepsilon}(\omega)$
- $\hat{\sigma}(\omega) = Re[\hat{\varepsilon}(\omega)] + i \cdot Im\left[\hat{\Phi}(\omega)\right]$

- Mechanical properties may be expressed in terms of

Complex Modulus $E^* = E' + iE''$

- **E': dynamic storage modulus ~ Young's modulus**
- **E'': dynamic loss modulus**
- **Loss Factor: $Q^{-1} = \tan\delta = E''/E'$ (account for anelasticity and dissipation)**

Advantages of DMA vs. static

- Information both in elastic and in viscous field
- Possibility to explore a range in frequency

DMA is thus particularly useful in the characterization of viscoelastic materials like organic tissues

Dynamic mechanical test

Complex modulus for indentation test

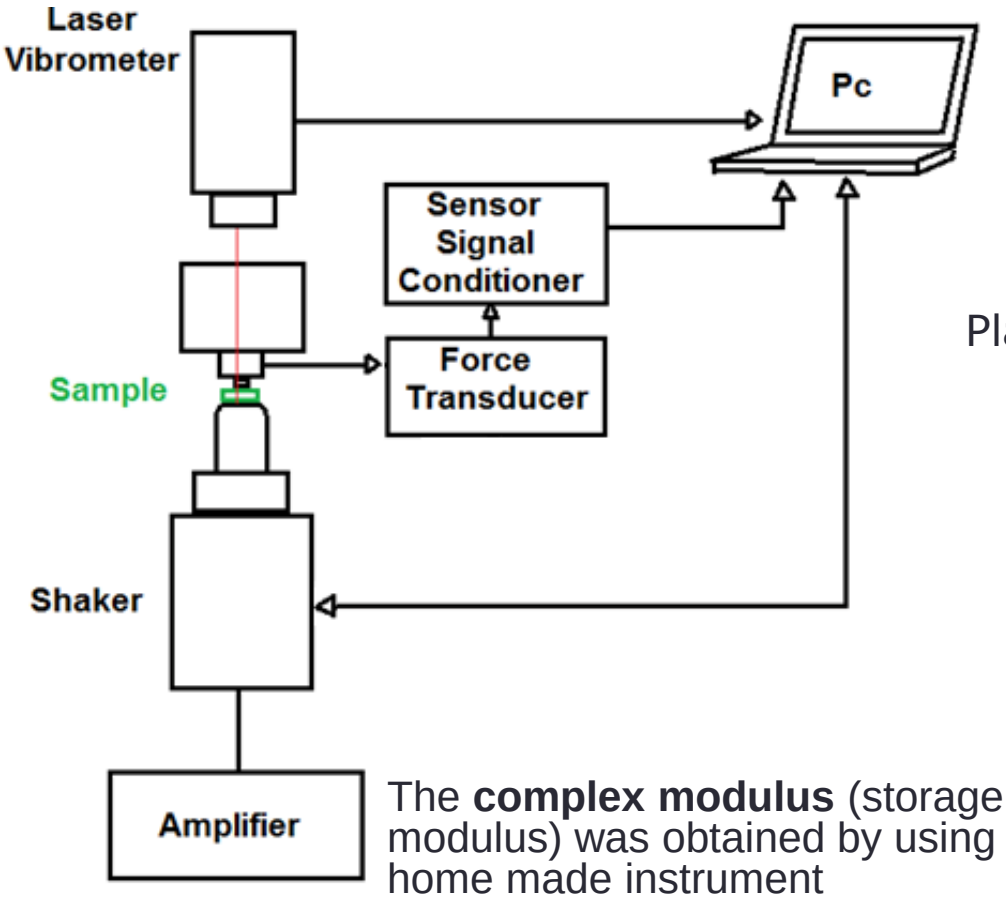

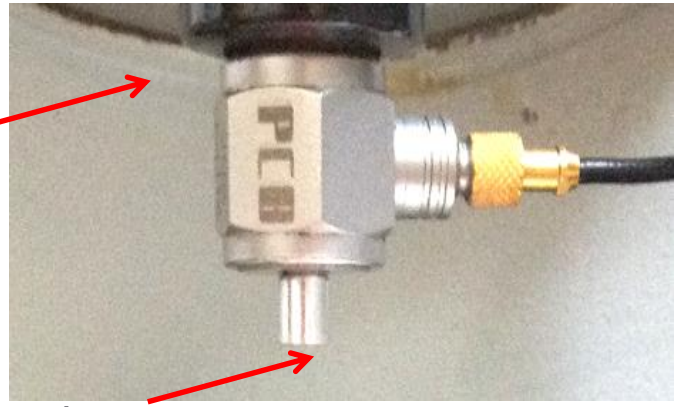

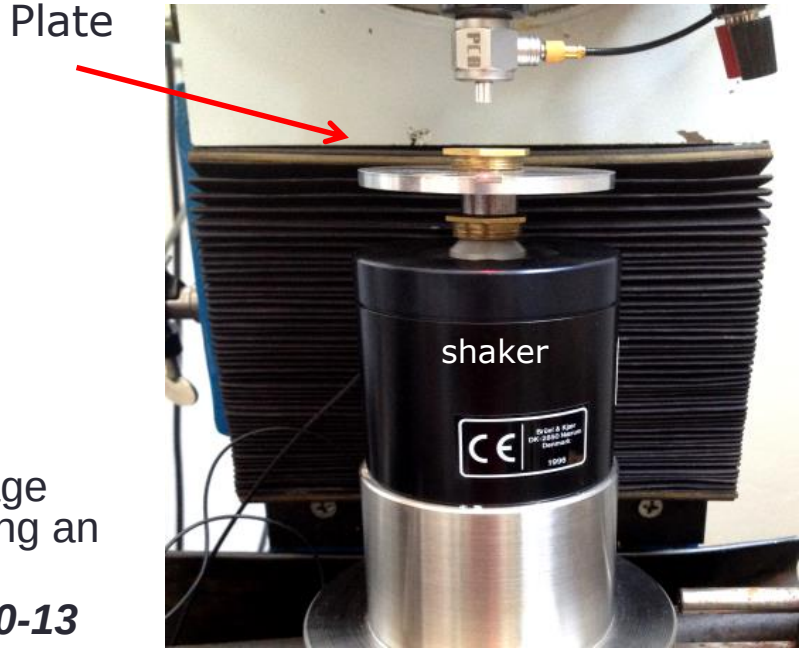

The **complex modulus** (storage modulus) was obtained by using an home made instrument

Project ROBOSKIN-FP7 2010-13

The Testing Methods I.

Dynamic tests (30 Hz) on cylindrical samples (diameter 4 mm) at different stretch and in maximum swelling conditions

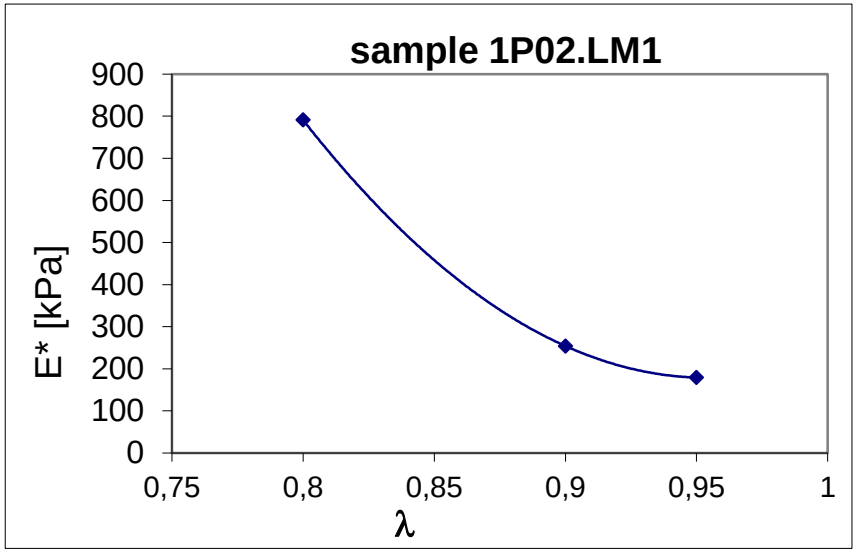

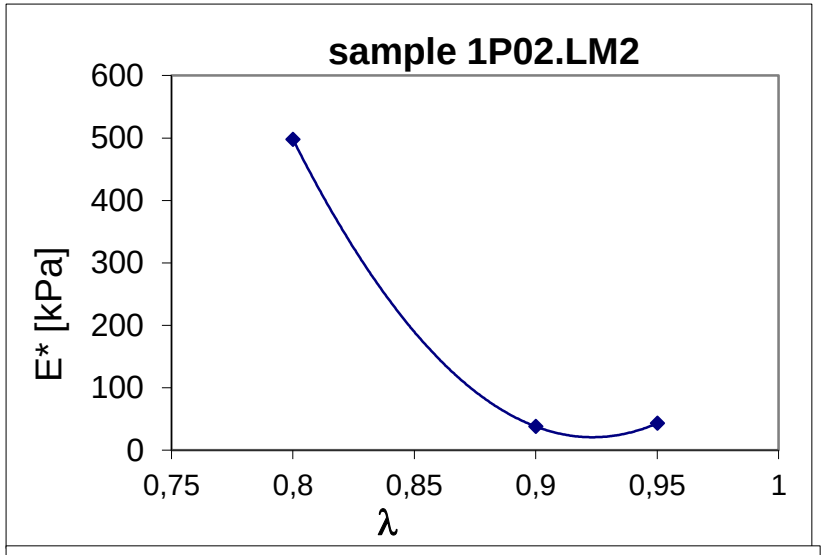

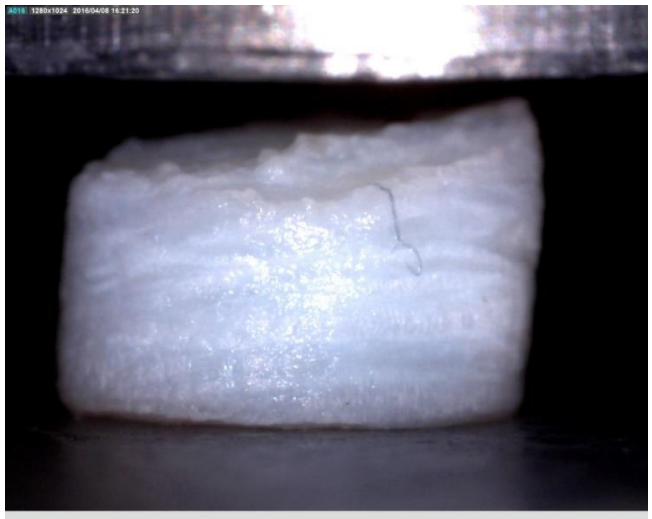

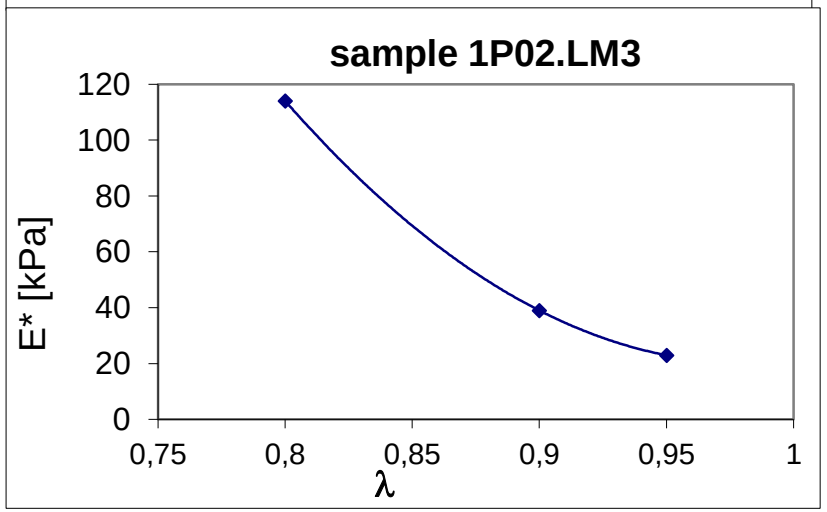

The Testing Methods

II - Indentation method

Radial cross sections were cut from anterior, central and posterior zones.
From each slice different sites on the section were investigated

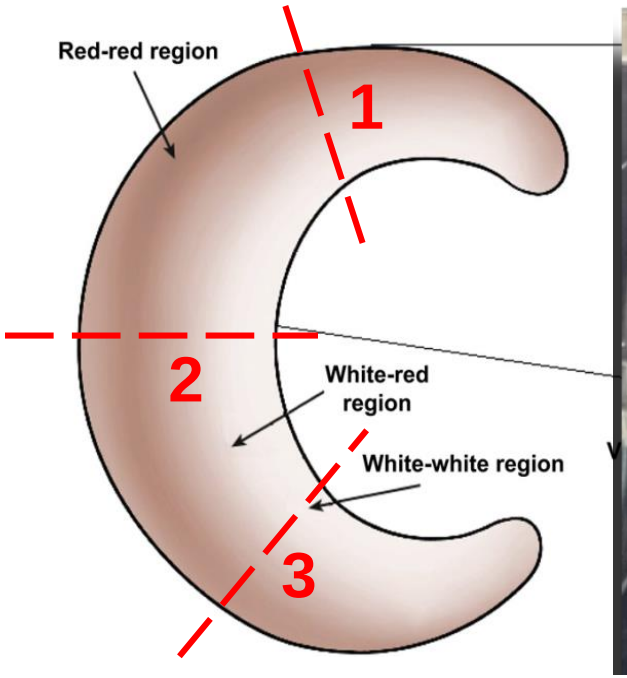

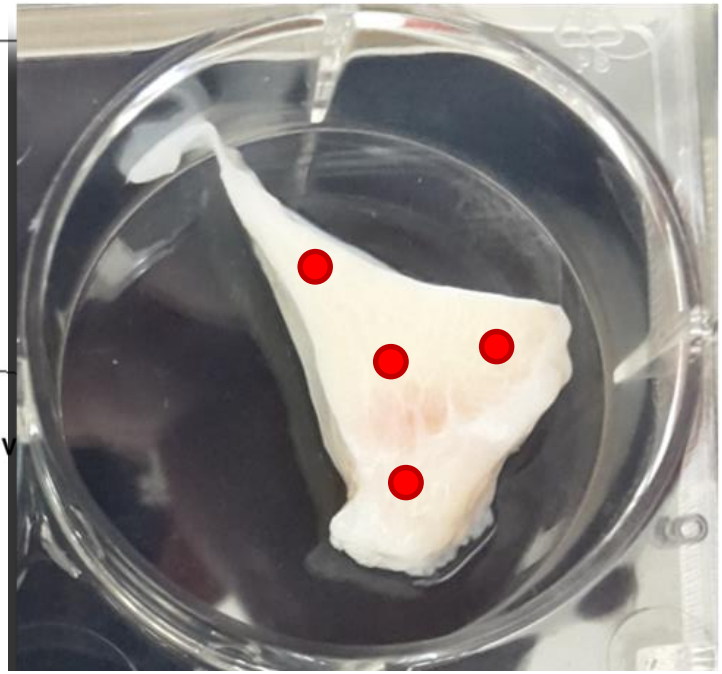

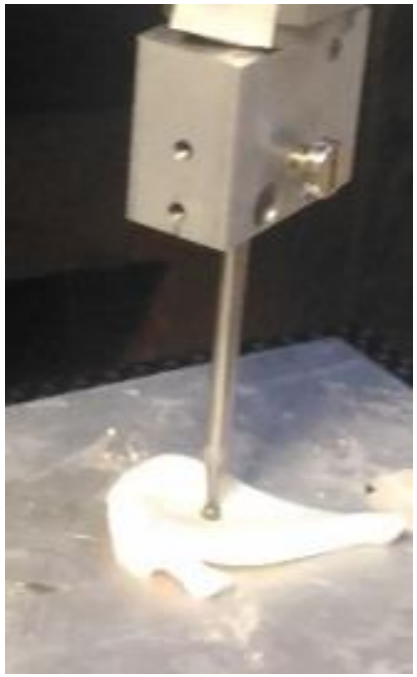

Region 1: anterior
Region 2: central
Region 3: posterior

The Testing Methods II.

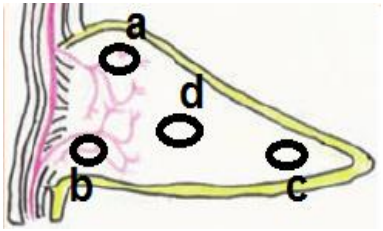

Cross-sections Lateral Meniscus

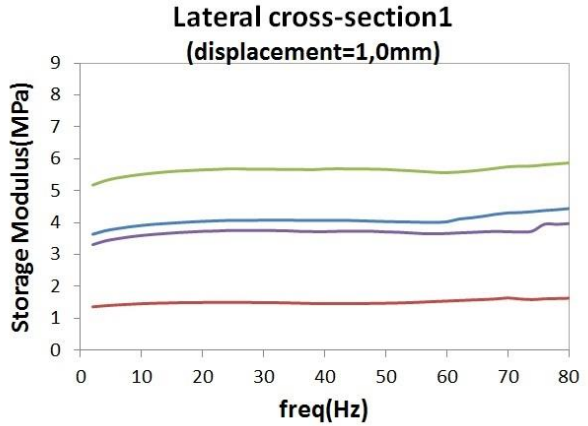

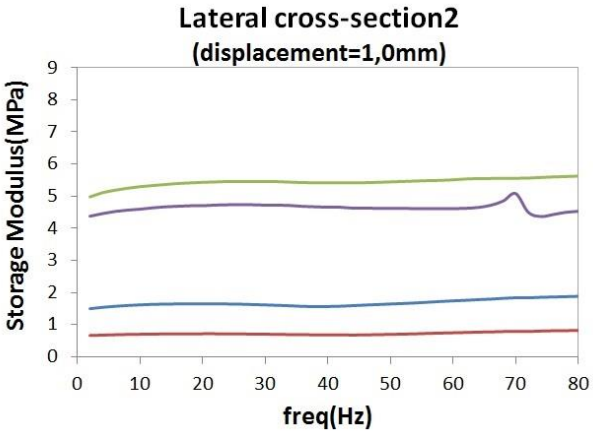

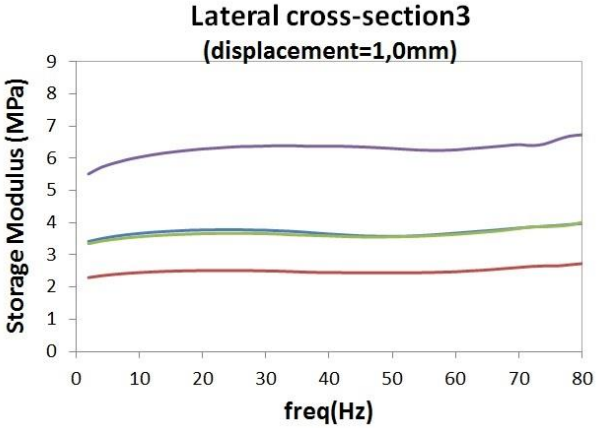

The Testing Methods II.

Indentation method: advantages

- test specimen of definite shape not required
  very important asset in the effort of testing the tissue as close as possible to its undisturbed state

- Localization of the measurement can be varied at leisure by changing the size of the indenter (mm to μm)
  The region over which the properties of the tissue are averaged by an indentation test is the stressed zone under the indenter, which has a size of the order of the tip diameter in the case of indentation by a cylinder, or the diameter of the contact area in the case of a spherical tip

The Testing Methods II.

Indentation method: problems

- No direct evaluation of the compressive Young modulus

  the relation of the modulus with the measured elastic deformation of the indented surface is provided by the theory of elasticity, which normally assumes a linear homogeneous and isotropic material.

- Unknown uncertainties introduced by large deformations, anisotropy and local inhomogeneity

- Partial alteration of the internal structure due to the cut of the fibrils

The Composite Structure

1. External mat
2. Radial Collagen fibrils
3. Circumferential Collagen fibrils

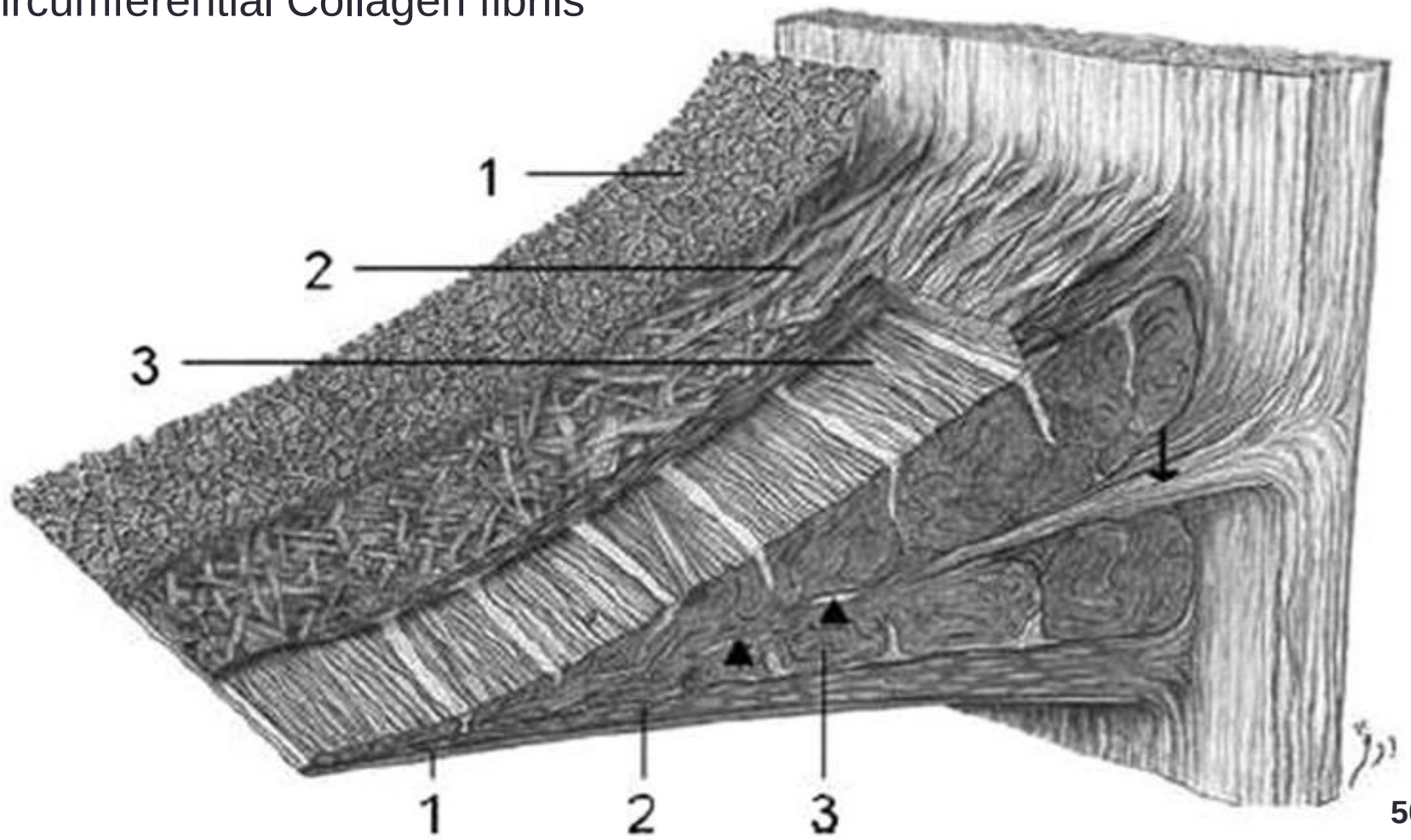

The Testing Methods III.

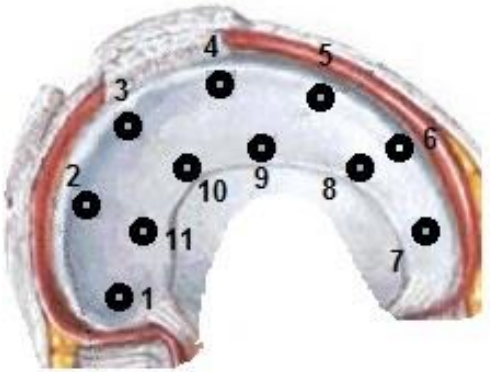

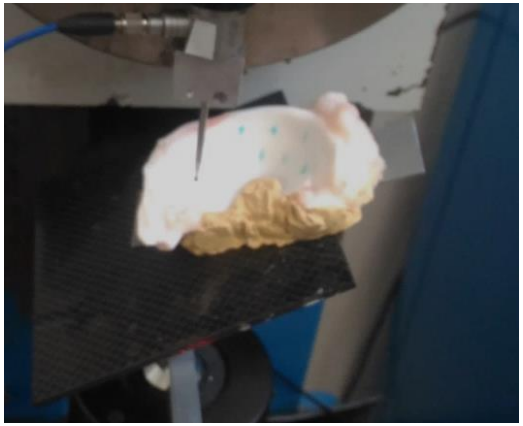

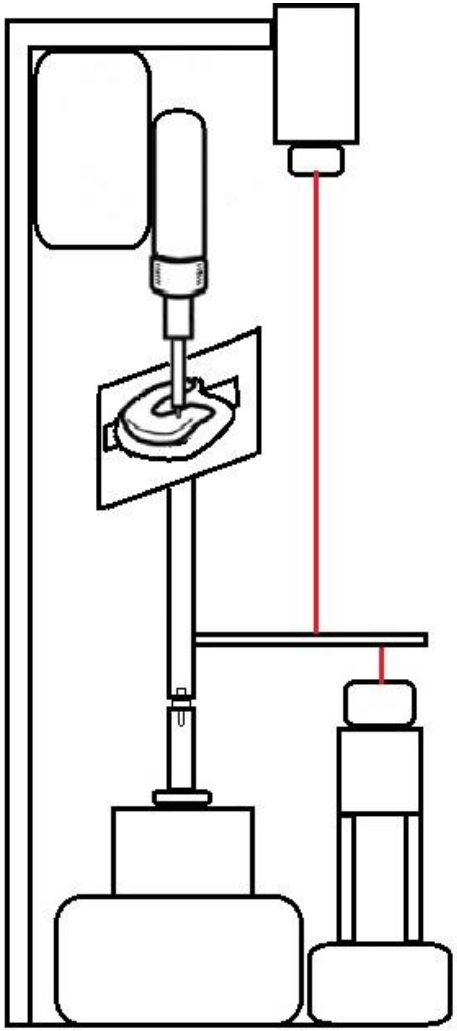

The Testing Methods III.

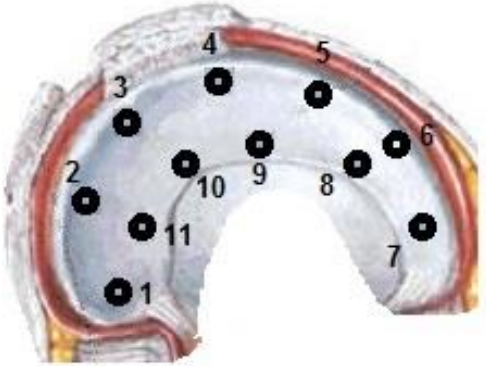

Intact Lateral Meniscus

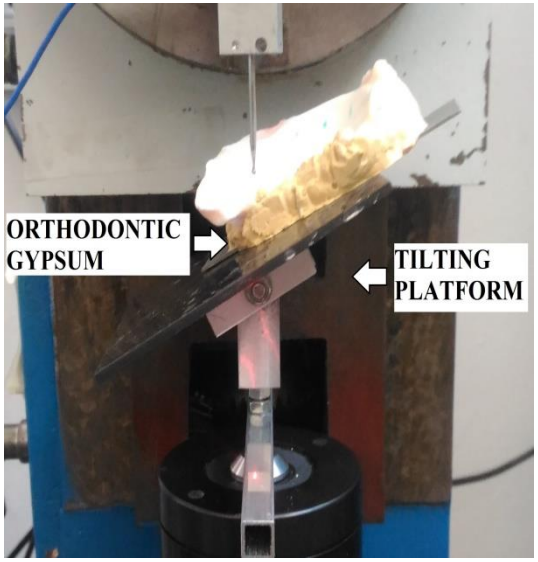

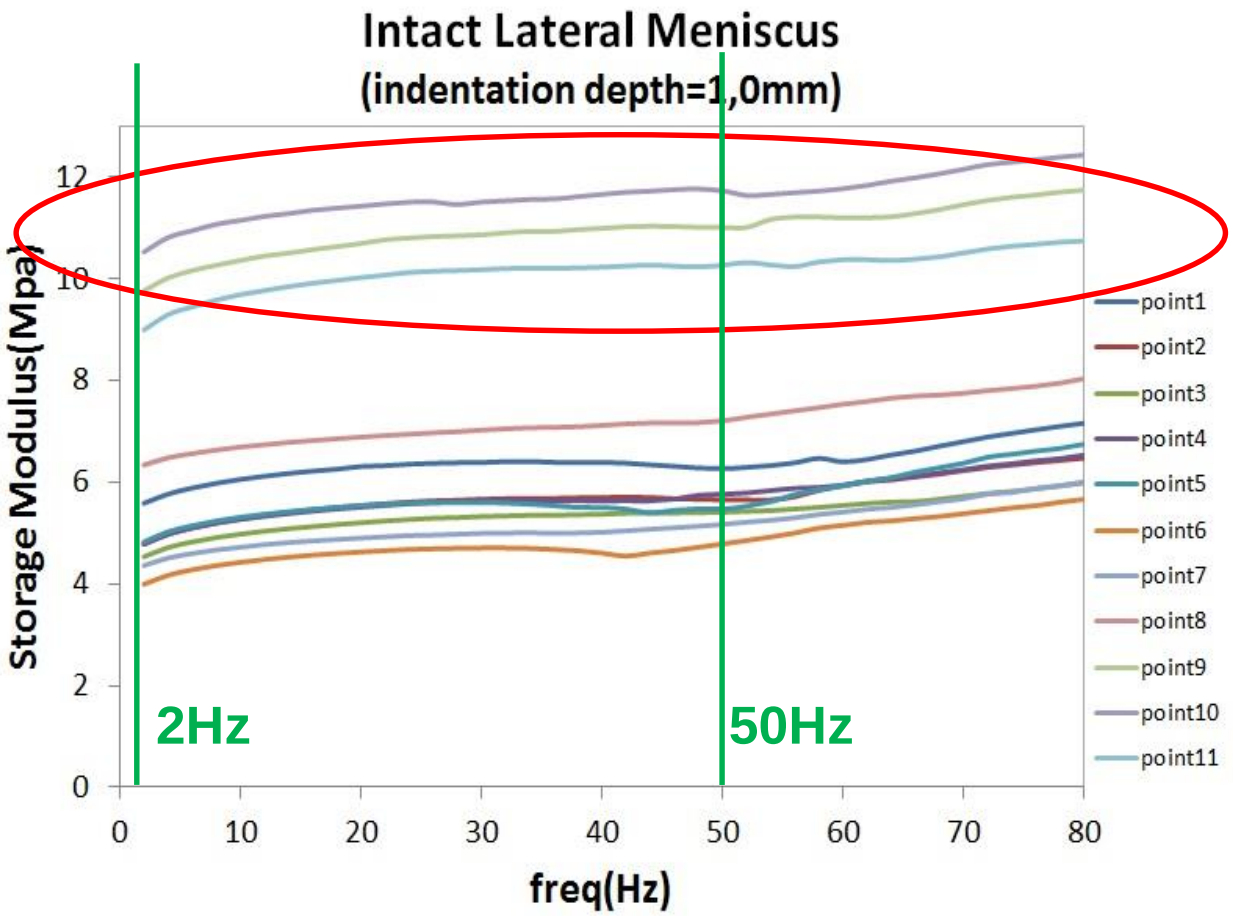

The Testing Methods III.

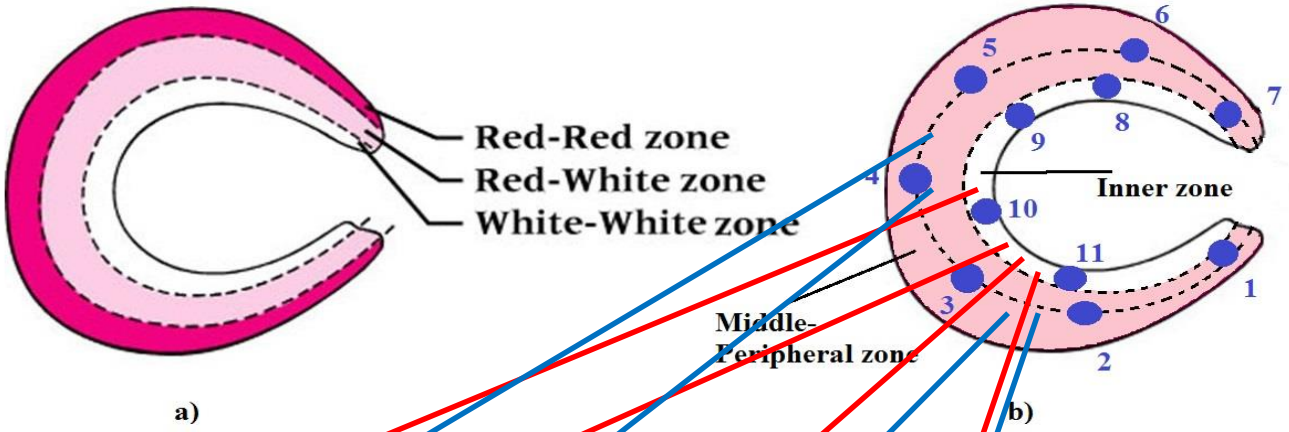

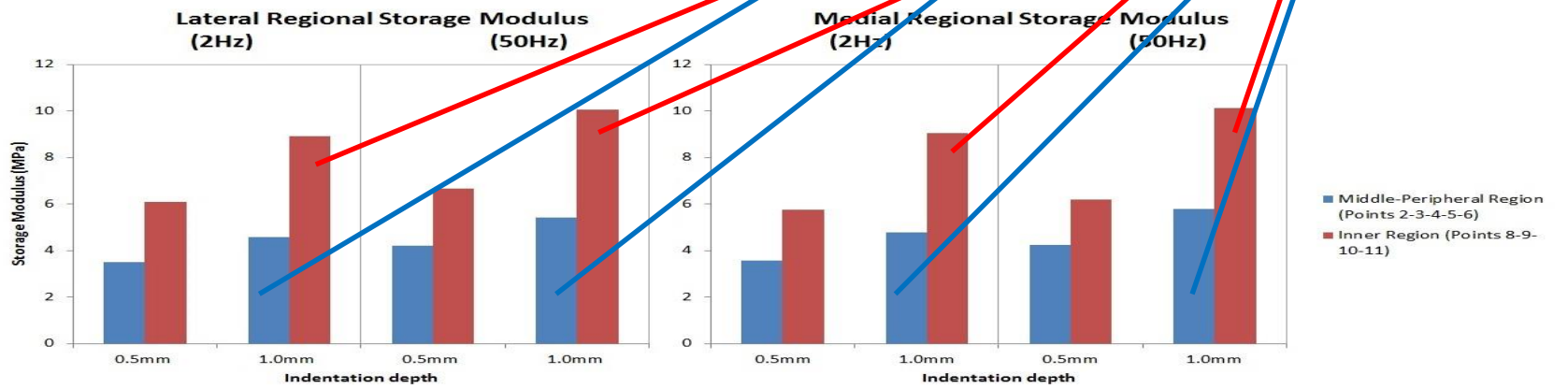

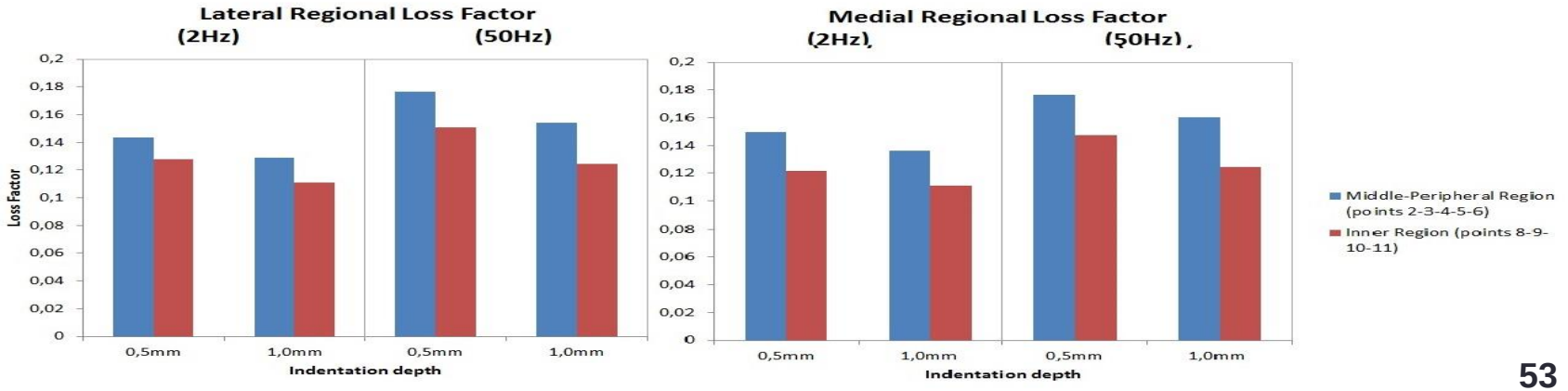

Conclusions

Natural Composite Material analysis is a quite complex task, highly dependent upon:

- The samples homogeneity and availability
- The sampling procedure and technologies
- The load conditions
- The storage protocol

A conservative approach consisting in the maintenance of the **natural condition** of the biological tissue are fundamental to observe the effective mechanical response of the material

- perfusion of the sponge-tissue for the liver
- continuity of fibers for the meniscus

Zwick / Roell

esaote

INTERNATIONAL Piezosurgery Academy

FINCANTIERI MARINE GROUP

D'APPOLONIA

National Research Council of Italy

IEIIT

Institute of Electronics, Computer and Telecommunication Engineering

mectron medical technology

Columbus Superconductors

KING'S College LONDON

UNIVERSITEIT GENT

BASF

BASF Polyurethanes Europe

Camelot biomedical systems

NANOJANUA

CMM FBK

CENTER FOR MATERIALS AND MICROSYSTEMS

UNIVERSITÀ DI TRENTO

UNIVERSITÀ DEGLI STUDI DI GENOVA

UNIVERSITÀ DEGLI STUDI
DI GENOVA

Prof. Marco Capurro

Acknowledgments:

Zwick / Roell

Dr. Elisabetta Monteleone
Sig. Massimiliano Varriale